Journal of Materials Chemistry A

REVIEW

View Article Online
View Journal | View Issue

Cite this: J. Mater. Chem. A, 2025, 13, 136

Solid-state organic electrochemical transistors (OECTs) based on gel electrolytes for biosensors and bioelectronics

Dongdong Lu * and Hu Chen *

Organic electrochemical transistors (OECTs) have emerged as promising platforms for biosensors and bioelectronic devices due to their biocompatibility, low power consumption, and sensitivity in amplifying chemical signals. This review delves into the recent advancements in the field of biosensors and bioelectronics utilizing solid-state OECTs with flexible gel electrolytes. Gel electrolytes, including hydrogels and ionic liquid gels, offer improved mechanical compatibility and stability compared to traditional liquid electrolytes, making them suitable for wearable and implantable biosensing applications. We explore the properties and classifications of gel electrolytes for OECTs, highlighting their self-healing, responsive, temperature-resistant, adhesive, and stretchable characteristics. Moreover, we discuss the application of solid-state OECTs based on gel electrolytes in ion sensing, metabolite detection, and electrophysiological sensing. Despite significant progress, challenges such as manufacturing scalability and the development of responsive OECTs persist. Future directions involve leveraging the multi-responsiveness of hydrogel electrolytes for intelligent sensor designs, integrating solid-state OECTs with energy storage devices for self-powered applications, and advancing wireless communication functionalities for real-time health monitoring. This comprehensive overview provides insights into the potential of solid-state OECTs based on gel electrolytes and outlines future research directions in biosensing and bioelectronics.

Received 30th July 2024
Accepted 18th November 2024

DOI: 10.1039/d4ta05288a

rsc.li/materials-a

1. Introduction of OECTs

Owing to their biocompatible nature, low energy consumption, and minimal operational voltage, organic electrochemical transistors (OECTs) have become highly regarded as potential

Dongguan Key Laboratory of Interdisciplinary Science for Advanced Materials and Large-Scale Scientific Facilities, School of Physical Sciences, Great Bay University, Dongguan, Guangdong, 523000, P. R. China. E-mail: ludongdong@gbu.edu.cn; chenhu@gbu.edu.cn

Dongdong Lu

Dongdong Lu obtained her PhD degree (2020) in polymer science and engineering from the University of Manchester (UOM), United Kingdom. She worked as a postdoc in materials science and engineering at the Southern University of Science and Technology (SUST) from 2020 to 2022. Now she is a researcher of School of Physical Sciences at Great Bay University (GBU). Her current research focuses on design, synthesis and fabrication of multi-functional polymers, nanomaterials, microgels and hydrogels used in fluorescent sensors and flexible electronics.

Hu Chen

Hu Chen has been a principal investigator at Great Bay University in China from 2022. He obtained his PhD from Peking University and received intensive training in organic synthesis in 2014. He subsequently joined Professor Iain McCulloch's group to focus on organic electronics. His current research centers on designing and synthesizing high-performance innovative organic semiconductors as well as device fabrication and characterization.

options for advancing biosensors and bioelectronic devices.[1–4] OECTs exhibit high transconductance, facilitating sensitive amplification of chemical signals, thus holding significant potential across various biomedical applications, including ion sensing,[5,6] DNA detection,[7] alcohol sensing,[8] metabolite detection,[9] and cell detection.[10,11] Traditional OECTs consist of three-terminal devices with source, drain, and gate electrodes.[12] An organic semiconductor layer serves as a conducting channel, isolated from the gate electrode by an ion-conducting electrolyte. OECT operation relies on interplay between ion and charge transport, resulting in modulation of the current (I_{DS}) flowing from the source to the drain through the conducting channel.[1] The transconductance parameter (g_m) is used to evaluate the amplification characteristics of OECTs, crucial for enhancing sensing performance, characterized by the detection limit (LOD, signal-to-noise ratio ≥3).[13,14]

$$g_m = \frac{\partial I_D}{\partial V_G} = \frac{Wd}{L}\mu_n C^*(V_{th} - V_G) \quad (1)$$

In this equation, W, L, and d denote the channel width, length, and thickness, respectively; μ, C^*, and V_{th} are the carrier mobility, volume capacitance, and threshold voltage of the active layer, respectively. High-performance OECTs can be achieved by optimizing the geometry of devices based on an Organic Mixed Ionic-Electronic Conductor (OMIEC) or μC^* values,[15,16] as indicated by eqn (1).[17,18]

Currently, research on OECTs predominantly centers on the study of active materials, electrolytes, interface modification, and the optimization of device geometry. Enhancing electronic properties of OMIECs, such as high mobility and large capacitance, is crucial for achieving high-performance OECTs.[17,19] Notably, poly(3,4-ethylenedioxythiophene)-poly(styrene sulfonate) (PEDOT:PSS) has exhibited a maximum μC^* product of 1500 F cm^{-1} V^{-1} s^{-1} due to its exceptional conductivity properties.[17] This achievement is based on the original hole current of PEDOT:PSS of OECTs reaching its maximum value at zero gate bias. When applying a positive gate voltage, cations (*e.g.*, Na^+, K^+, and Li^+) from the electrolyte move into the organic channel, leading to de-doping of PEDOT through electrochemical reactions as shown in eqn (2). As highly conductive $PEDOT^+$ is reduced to non-conductive $PEDOT^0$, the device's drain current decreases, demonstrating typical depletion-mode transistor behavior.[16] Additionally, multifunctional OECTs employ various strategies, including interface modification and functional materials, to modulate the OECT ion circuit and manipulate charge transport within the channel.[20,21]

$$PEDOT^+:PSS^+ + M^+ \leftrightarrow PEDOT^0 + M^+:PSS^- + h^+ \quad (2)$$

While liquid electrolyte-based OECTs have been prevalent, their liquid nature presents challenges such as leakage, evaporation, environmental contamination and electrolyte electrolysis, hindering long-term stability and performance.[22–24] To address these issues, solid-state OECTs have emerged as a promising alternative, particularly suitable for wearable biosensing and flexible electronic applications.[25–27] Solid-state electrolytes facilitate large-scale manufacturing of compact and highly integrated OECTs using simple printing techniques.[28] Moreover, they provide superior flexibility and durability[27] by enabling the devices to withstand daily wear and mechanical stresses.[29,30]

2. Gel electrodes

Gels, characterized by cross-linked three-dimensional polymer networks, possess a unique ability to swell in liquid electrolytes, effectively absorbing and immobilizing them. This distinctive property combines the high ion conductivity of liquid electrolytes with the processability of solid electrolytes, thereby addressing concerns related to liquid leakage. Furthermore, the high hydration capacity of gels facilitates ion transport, ensuring compatibility with biological tissues.[31] Notably, their mechanical properties closely resemble those of human tissues, with Young's modulus ranging from 1 Pa to 300 MPa, covering the ranges of skin and muscle (200–500 kPa) and brain tissue and spinal cord (500 Pa–200 kPa).[32] This mechanical compatibility with soft tissues makes hydrogels an ideal choice for implants and wearable bioelectronics.[33] The gel electrolytes utilized in OECTs are typically classified into two categories: hydrogels and ionic liquid gels (IL gels). This review specifically hones in on the classification and properties of gel electrolytes, and summarizes the progress of gel electrolyte-based OECT applications in the fields of biosensing and bioelectronics (Fig. 1). Furthermore, the review provides an overview of the existing challenges encountered in this field and proposes future research directions to address them effectively.

2.1 Categories of gel electrodes

2.1.1 Hydrogels. Hydrogels, characterized by their three-dimensional cross-linked polymer networks, offer a versatile platform with tunable physicochemical properties such as biocompatibility, biodegradability, material transport, and mechanical strength.[45] These properties make them conducive to loading and delivering cells, drugs and growth factors, thereby facilitating cell adhesion and proliferation.[46–48] Hydrogels primarily conduct protons, with ion transport facilitated by the diffusion of intramolecular and intermolecular hydrogen bonds within the polymer matrix or residual free volume water.[49] Studies have demonstrated that increasing glycerol concentration can enhance hydrogel ion conductivity.[50,51] Consequently, solid-state OECTs employing various hydrogel electrolytes have been developed for applications in biosensing,[41] synaptic neural simulation,[52] and bioelectronics.[53] Examples of synthesized hydrogel electrolytes include poly(ethylene glycol) (PEG),[54] poly(*N*-isopropylacrylamide) (PNIPAm),[55] poly(hydroxyethyl acrylate) (PHEA),[56] poly(hydroxyethyl methacrylate) (PHEMA),[57] and poly(vinyl alcohol) (PVA).[38] These hydrogels offer excellent controllability, ease of design, and mechanical properties that can be tailored to mimic natural tissues, thereby reducing interface resistance and enhancing compliance with biological systems.

Natural hydrogels, including gelatin,[37] chitosan,[43] agar, *etc.*, derived from biomaterials offer distinct advantages compared

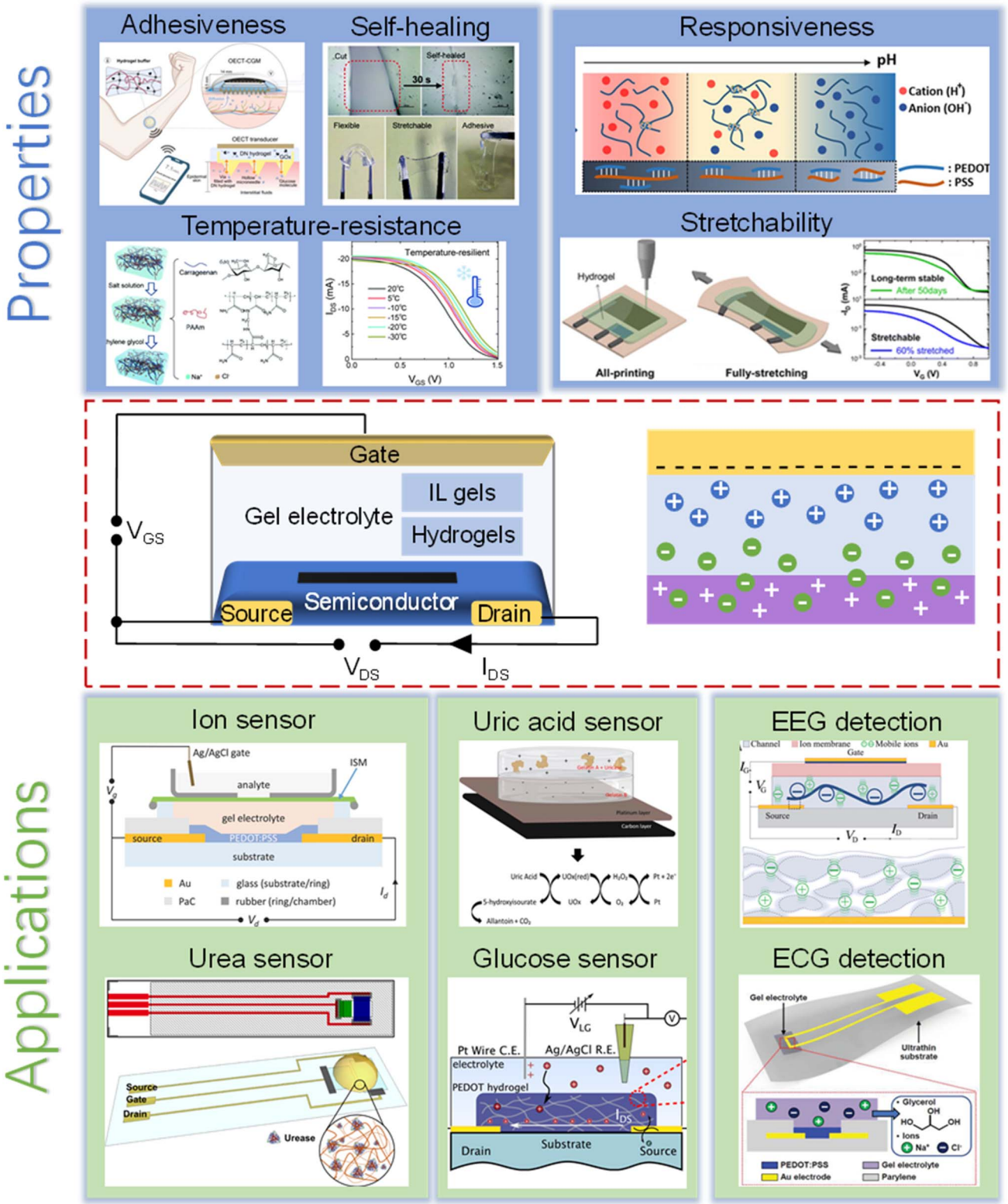

Fig. 1 Schematic illustration of the advancement of gel electrolyte-based OECTs in terms of their characteristics and diverse applications. Reproduced from ref. 34–44; Copyright 2020, American Chemical Society;[35] Copyright 2018, American Chemical Society;[37] Copyright 2021, American Chemical Society;[36] Copyright 2024, AAAS;[34] Copyright 2023, Royal Society of Chemistry;[38] Copyright 2014, Wiley-VCH;[39] Copyright 2018, IOP publishing, Ltd;[40] Copyright 2020, Wiley-VCH;[41] Copyright 2022, American Chemical Society;[42] Copyright 2019, AAAS;[43] Copyright 2019, Wiley-VCH.[44]

to their synthetic counterparts, including inherent biocompatibility, low cytotoxicity, and environmental friendliness. However, they may exhibit weaker mechanical structures and susceptibility to degradation. It is imperative to maintain precise control over the molecular weight and composition of the polymer in order to align with the specific demands of solid-state OECTs, including biomechanical properties and gel behavior. Composite hydrogels combine natural and synthetic materials, and offer enhanced mechanical properties and biocompatibility, presenting promising avenues for future research. For example, Liu *et al.* reported OECTs based on a dual-network antifreeze hydrogel, comprising cross-linked polyacrylamide (PAAm) and carrageenan. This innovative hydrogel demonstrated remarkable attributes including biocompatibility, mechanical strength, antifreeze properties, and high ion conductivity, enabling operation at −30 °C.[36,58] However, the preparation methods for these hydrogel electrolytes commonly involve swelling in salt solutions (*e.g.*, sodium chloride or phosphate-buffered saline) to enhance ion conductivity. Nevertheless, this structure is susceptible to deformation at elevated temperatures and after prolonged use. Moreover, water evaporation can diminish the free volume conduction path of ions, leading to performance degradation in hydrogel-based OECTs.

2.1.2 Ionic liquid gels. Ionic liquid gels (IL gels), comprising non-volatile ionic liquids with low melting points below 100 °C, have emerged as an alternative to hydrogels, particularly for flexible electronic devices,[59] biosensors[60,61] and solid-state OECTs.[62] IL gels offer advantages such as minimal vapor pressure, high thermal stability, and superior ionic conductivity.[63] Numerous studies have delved into the synthesis of ionic gels, elucidating ion transport mechanisms and the dynamics of ion/electron interface transport.[64] These investigations have significantly enhanced the understanding of ionic gels across various relevant fields.[65,66] Common ionic liquids used in IL gels include 1-ethyl-3-methylimidazolium ethylsulfate ([C_2MIM][$EtSO_4$]), 1-butyl-3-methylimidazolium bis(trifluoromethylsulfonyl)imide ([BMIM][TFSI]), and 1-ethyl-3-methylimidazolium bis(trifluoromethylsulfonyl)imide ([EMIM][TFSI]). However, their toxicity and high fluoride content limit direct contact with skin and the environment.[55,67] Biocompatible ILs containing choline cations and amino acids or carboxylic acids as anions (*e.g.*, choline lactate ([Ch][Lac]) or choline glycolate ([Ch][Glyco])) have been developed,[68,69] offering high ionic conductivity, biocompatibility, and environmental stability.[70,71] These materials hold promise for implementing all-solid-state OECTs in long-term biomedical applications such as skin electrophysiology monitoring.

2.2 Properties of gel electrolytes

The unique properties and advantages of gel electrolytes provide OECTs with several critical functionalities. Hydrogels have highly tunable physical and chemical properties. Their conductivity, mechanical strength, and biocompatibility can be precisely controlled by altering their composition and structure.[72,73] This tunability allows OECTs to meet various application requirements, enabling highly customized sensor designs. Due to their softness, gel electrolytes combined with OECTs can achieve greater mechanical flexibility and stability,[74] making them ideal for wearable and implantable applications. The high-water content of hydrogels provides exceptional ionic conductivity, allowing OECTs to operate efficiently at low voltages, enhancing electrochemical conversion efficiency and signal amplification.[11] The biocompatibility of hydrogels makes them particularly suitable for biomedical applications in OECTs. Hydrogels are not only compatible with biological tissues but also maintain stability in *in vivo* environments,[75] reducing potential irritation and immune responses.[76] This characteristic allows OECTs to play vital roles in real-time biosignal monitoring, drug delivery control, and implantable medical devices. Moreover, specially designed smart responsive and thermally stable hydrogel electrolytes can expand the application range of OECTs.[36,77,78] Responsive hydrogel electrolytes allow OECTs to quickly adjust their electrochemical properties to changes in the external environment, achieving high-sensitivity and rapid-response sensing applications. Thermally stable hydrogels maintain their structural and functional integrity at high or low temperatures, ensuring consistent operation. This thermal stability ensures that OECTs maintain their performance under various environmental conditions, preventing degradation or failure due to temperature fluctuations. This characteristic is particularly advantageous for biomedical devices and sensors operating in complex environments. This chapter discusses the research progress of solid-state OECTs based on gel electrolytes from the perspectives of conductivity, volumetric capacitance, self-healing, stretchability, responsiveness, temperature-resistance, and self-adhesion.

2.2.1 Conductivity and volumetric capacitance. In eqn (1), as introduced in the OECT discussion, the parameter μC^* represents a key intrinsic property of OECTs. In this expression, μ denotes the charge carrier mobility, a measure of how easily charges move through the material, while C^* stands for the volumetric capacitance, which reflects the ability of the material to store charges per unit volume. Together, the μC^* product determines the overall transconductance and performance of the OECT, influencing the sensitivity and amplification of the device in biosensing applications. The μC^* value is a fundamental factor in the design and optimization of OECTs, as it directly relates to the efficiency of ion–electron coupling and signal transduction within the device. By maximizing both the mobility (μ) and capacitance (C^*), high-performance OECTs can be achieved, which are essential for applications requiring fast, sensitive detection and stable operation at low voltages. Optimizing the μC^* value, therefore, is crucial for advancing the application of OECTs in bioelectronics, particularly in real-time health monitoring and biosensor technologies.

The extraction of electronic mobility in OFETs is well-established, but applying similar techniques to OECTs is challenging due to the presence of both ionic and electronic charges in the OECT channel. Moreover, the mobility in OECTs can be voltage-dependent due to variations in electronic charge density across the film, resulting from changes in the electrochemical

potential from the source to the drain. At high doping potentials, electronic charges can saturate available states (HOMO or LUMO), reducing the efficiency of charge transport. To determine the capacitance of materials used in OECTs, electrochemical impedance spectroscopy (EIS) is frequently employed. The typical EIS setup involves a three-electrode system, with the OMIEC film serving as the working electrode, alongside a reference electrode and counter electrode. The counter electrode must possess a significantly larger capacitance than the working electrode to ensure it doesn't hinder the reactions occurring at the working electrode. The process involves applying a small alternating current modulation across a range of frequencies (typically from 10^6 to 10^{-1} Hz) on top of a direct current offset. Once the impedance data are collected, capacitance (C) can be extracted, typically at lower frequencies where ionic movement is slower and more capacitive behavior is observed.

Capacitance can also be derived through cyclic voltammetry. In the absence of faradaic reactions, the voltammogram can be integrated to estimate the volumetric capacitance, assuming ideal capacitor behavior in the OMIEC film. This method closely aligns with the results from EIS.

However, if redox peaks are present, those areas are excluded to avoid skewing the capacitance calculation. Additionally, it is important to consider factors like scan rate, as overly fast scans may lead to underestimation of capacitance due to incomplete charging/discharging cycles. Lastly, for accurate results, capacitance should be measured for films of varying geometries, ensuring that the extracted values scale linearly with the film volume.

2.2.2 Self-healing properties. Incorporating self-healing materials into solid-state OECTs presents an intriguing avenue for creating devices with enhanced reliability and prolonged lifespans. However, the utilization of self-healing materials in OECTs is currently in its nascent stages. One of the primary challenges is to achieve effective repair performance while preserving the electronic/ion transport and mechanical properties of both the conjugated polymer and solid electrolyte, ensuring swift restoration to the original performance post-self-healing.

Fabio Cicoira's work revealed that PEDOT:PSS thin films underwent rapid electrical repair (approximately 150 ms) simply by wetting the damaged area with water.[79] Hydrogels, renowned for their self-healing properties, leverage dynamic bonding interactions such as dynamic covalent bonds,[80] hydrogen bonds,[81–83] ion bonds,[84] supramolecular host–guest interactions,[85] and hydrophobic interactions.[86] In addition, the high water content of the hydrogel can provide PEDOT:PSS with self-healing properties. Wei Lin Leong *et al.*[35] pioneered the development of a solid-state OECT endowed with self-healing capabilities and robust electrical performance. Their design utilized a PEDOT:PSS and surfactant Triton X-100 (PEDOT:PSS/TX) matrix as the channel, coupled with a poly(vinyl alcohol) (PVA) hydrogel as the electrolyte. The high ionic conductivity of the PVA hydrogel (9.8×10^{-3} S cm^{-1}) facilitated OECT operation by modulating PEDOT:PSS doping. The resulting PEDOT:PSS/TX-PVA based OECT exhibited an impressive peak transconductance (48.7 mS) and on/off ratio ($\approx$1500) (Fig. 2A). The TX functions as both an enhancer of electrical performance and a self-repairing agent. When the damaged area comes into contact with the PVA hydrogel, it triggers both physical and electrical self-repair of the PEDOT:PSS/TX film (Fig. 2B). Consequently, the OECT autonomously restored its initial performance to a range of 85–100% post-damage (Fig. 2C), with a transconductance of approximately 45 mS at $V_G = -0.075$ V and an on/off ratio of $\sim$1300 (Fig. 2D). Additionally, as an ion sensor, this OECT demonstrated the capability to detect Na^+.

2.2.3 Responsiveness. Environmental stimulus responsiveness is a compelling attribute of hydrogels, as they can dynamically adjust their properties (such as water content, surface charge, hydrophilicity–hydrophobicity, and mechanical modulus) in response to various stimuli. These stimuli encompass chemical cues (*e.g.*, pH,[87] oxidizing agents,[88] ions,[89] and solvents[83]), biological signals (*e.g.*, enzymes[90] and antigens[91]) and physical factors (*e.g.*, light,[92] temperature,[93] magnetic fields,[94] electric fields,[95] and ultrasound[96]). Consequently, hydrogels find extensive utility across diverse fields, spanning drug delivery,[97] biosensors,[83] biomimetic materials,[87] and regenerative medicine.[98]

Tae-il Kim[37] pioneered the development of pH-responsive solid OECTs utilizing gelatin hydrogels. In this design, the transistor channel (PEDOT:PSS) and electrodes were fabricated on a flexible polyethylene terephthalate (PET) substrate. Gelatin served as a solid electrolyte medium, facilitating ion migration from the gate into the channel. The gelatin material was modified with acid and base additives to introduce mobile cations and anions, enabling their facile penetration into the PEDOT:PSS interface (Fig. 3A). Interaction with acidic and alkaline gelatin led to alterations in the chemical structure and conductivity of PEDOT:PSS channels. Specifically, acidic hydrogels enhanced the conductivity of PEDOT:PSS, leading to elevated output voltage (V_{out}) and gain, whereas alkaline hydrogels decreased conductivity, resulting in decreased V_{out} and gain (Fig. 3B). Integration of PEDOT:PSS with gelatin hydrogels under varying pH conditions allowed for modulation of OECT resistance, V_{out}, and gain. Notably, the maximum output voltage and gain of the inverter were governed by the pH conditions of the hydrogel, ranging from 1.1 to 0.46 V and 1.92 to 0.63 at pH = 1.13–13.43, respectively (Fig. 3C).

2.2.4 Temperature resistance. The application of hydrogel electrolytes in solid-state OECTs is hindered by temperature variations, as the inherent structure of hydrogel materials, predominantly water, renders them susceptible to temperature extremes. High temperatures accelerate water loss from hydrogels, while low temperatures cause freezing, both of which compromise their functionality. Additionally, dry environments can detrimentally affect the durability and conductivity of hydrogels. To enable continuous operation of solid-state OECTs under diverse temperature conditions, efforts have been directed towards enhancing the anti-freeze water-retention properties of hydrogel electrolytes.

Studies utilizing IL gels, such as [EMIM][TFSI],[99], [DEME][TFSI][100] and [EMI][TFSI][101]), have demonstrated improved stability of OECTs. For example, Someya and colleagues[44]

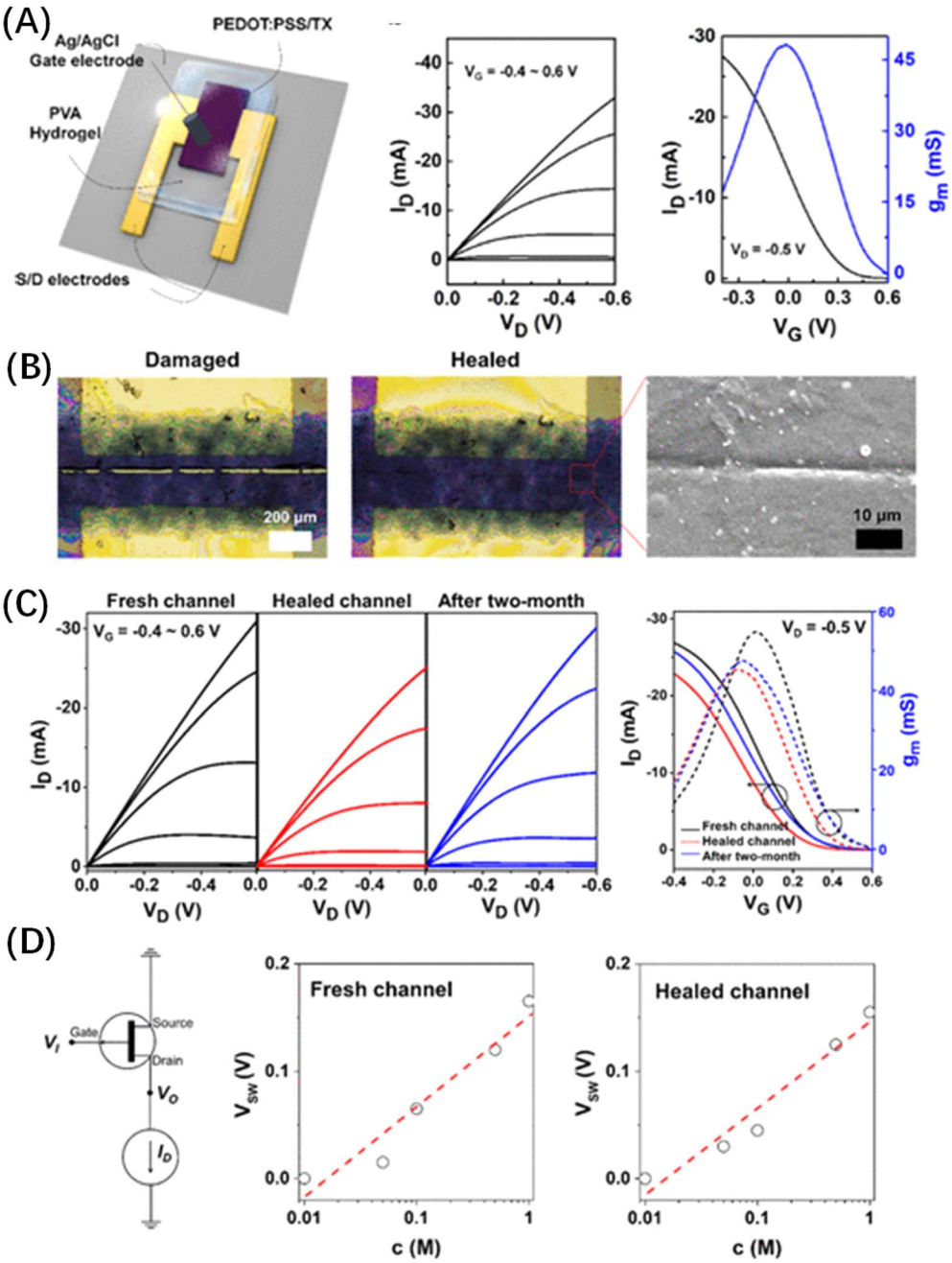

Fig. 2 (A) Schematic diagram of the PEDOT:PSS/TX-PVA based OECT and its output and transfer characteristics. (B) Optical and SEM images depicting the structural characteristics of damaged and healed PEDOT:PSS/TX channel layers. (C) Output and transfer characteristics of OECTs before and after self-healing. (D) Cumulative variation in the switching voltage of PEDOT:PSS/TX OECT *versus* Na^+ ion concentration before damage and after healing. Reproduced with permission.[35] Copyright 2020, American Chemical Society.

pioneered the utilization of non-volatile dilute IL gels as electrolytes in flexible OECTs, enabling continuous monitoring of electrocardiogram signals for over 3 hours with the device remaining functional for over a week. In 2023, Wei Lin Leong[78] and colleagues developed IL gel electrolyte consisting of poly(-vinylidene fluoride-*co*-hexafluoropropylene) (PVDF-*co*-HFP) and IL of 1-ethyl-3-methylimidazolium tetrafluoroborate (EMIM BF_4). The solid-state OECTs, constructed by using an active material (thiophene backbone functionalized with glycolated side chains (p(g1T2-g5T2)) and IL gel electrolyte (Fig. 4A(i)), exhibited great performance with a high transconductance of 220 ± 59 S cm^{-1}, an ultrafast device speed of 10 kHz, and excellent operational stability over 10 000 cycles (Fig. 4A(ii)). Due to the excellent thermal stability of the channel and electrolyte, the devices demonstrated reliable collection of electrophysiological signals even at extreme temperatures (−50 and 110 °C) (Fig. 4A(iii and iv)). Its transient speed was approximately twice as fast as those operating in 0.1 m NaCl electrolyte,

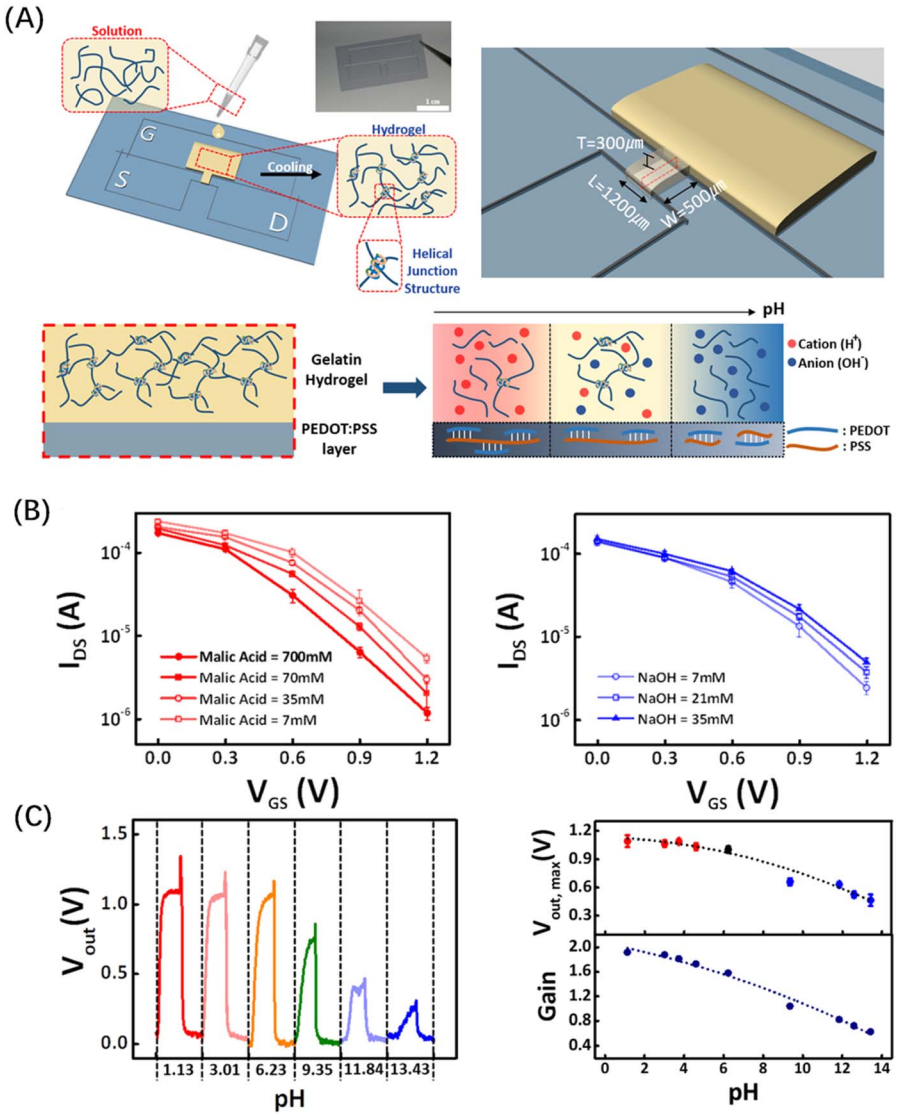

Fig. 3 (A) Gelatin based-OECTs and their sensitivity to pH. The manipulation of mobile ion concentration and polymeric chains in the gelatin-OECT is achieved through the introduction of acidic and basic substances to the original gelatin composition. (B) Transfer curves of gelatin based-OECTs with changing pH. (C) The pH-dependent characteristics of the maximum output voltage ($V_{out,max}$) and gain of the inverters with the gelatin based-OECTs. Reproduced with permission.[37] Copyright 2018, American Chemical Society.

benefiting from the low hydration level of the doping anions in the IL gel electrolyte. However, IL gels still exhibit drawbacks including biotoxicity, high cost, and slow ion diffusion.[102]

Inspired by biological synapses, Chuan Liu and colleagues[36] devised a hydrogel-based electrochemical transistor (HECT) featuring a transmission-like process (Fig. 4B(i)). A dual-network (DN) hydrogel composed of PAAm and carrageenan was synthesized *via* a one-step free radical polymerization. Sequential immersion in $NaCl_{(aq.)}$ and ethylene glycol endows it with great electrical performance and long-term stability, facilitating rapid self-repair, anti-freezing, and water-retention properties (Fig. 4B(ii and iii)). The HECT exhibited excellent biocompatibility and could operate effectively under harsh conditions for over 4 months at as low as −30 °C (Fig. 4B(iv and v)). Moreover, the self-healing capability of the hydrogel allowed for the full restoration of HECT electrical performance, showcasing the device's resilience against accidental damage (Fig. 4B(vi)). Similarly, Chuan Liu and colleagues[58] developed anti-freeze and water-retaining DN hydrogel electrolytes for solid-state dual-channel OECTs (Fig. 4C(i)). These hydrogel electrolyte possess good biocompatibility, high ionic conductivity, and stable operation across a wide temperature range from room temperature to −30 °C (Fig. 4C(ii and iii)). Furthermore, the devices can continuously monitor ion movement during OECT operation through transient current detection and *in situ* multipoint dynamic measurements of central potential (Fig. 4C(iv and v)).

2.2.5 Self-adhesiveness. Self-adhesiveness is a critical property of hydrogels for various applications, including bioelectronic sensors, and tissue engineering and repair. It ensures

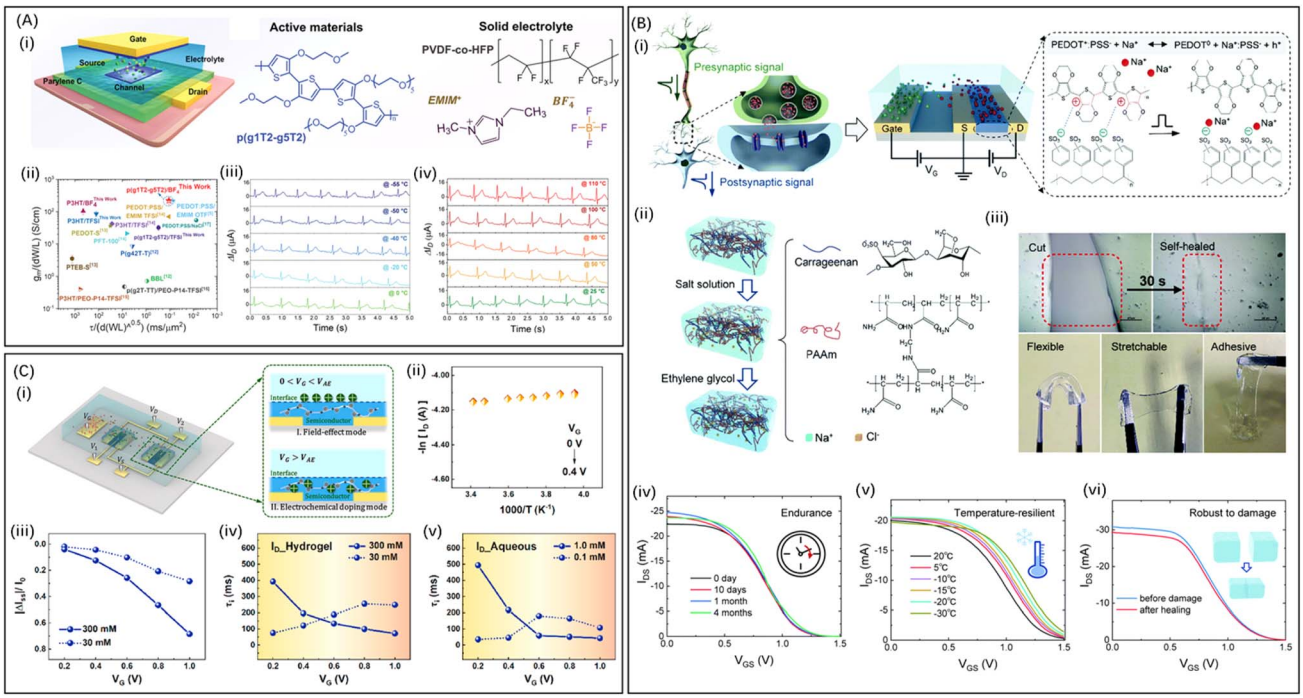

Fig. 4 (A) Schematic of solid-state OECTs constructed by using active materials of p(g1T2-g5T2) and IL gel electrolyte (i). (ii) Comparisons of OECTs in this work with previously reported ones in terms of steady- and transient-state performance. (iii) and (iv) ECG signals acquired by OECTs at extreme temperatures. Reproduced with permission.[78] Copyright 2023, Wiley-VCH. (B) The schematic illustration and characterization of a DN hydrogel-based HECT. Schematic illustration of the DN hydrogel-based HECT (i) and (ii). (iii) Optical microscope images and photos of the damaged and healed DN hydrogel electrolyte. The stability of the electrical properties of the DN hydrogel-based HECT including transfer characteristics evaluated over time (iv), at different temperatures (v) and in damaged and healed states (vi). Reproduced with permission.[36] Copyright 2021, Royal Society of Chemistry. (C) The schematic illustration and characterization of DN hydrogel-based dual-channel OECTs. (i) Schematic structure of the DN hydrogel-based dual-channel OECTs. (ii and iii) Temperature dependence of dual-channel OECTs at various electrolyte concentrations. (iv and v) Drain current behaviour under pulsed gate excitation with hydrogels containing various $KCl_{(aq.)}$ concentrations. Reproduced with permission.[58] Copyright 2022, Elsevier.

stable contacts between hydrogel devices and tissues, thereby enhancing overall performance.[103–105] Achieving adhesion involves introducing physical interactions and chemical bonds between hydrogels and substrates, including hydrogen bonding, hydrophobic interactions, metal complexation, π–π stacking, cation–π interactions, and covalent bonding.[106,107] Hydrogel electrolytes with high adhesive strength facilitate full contact with the channel, enabling effective ion penetration and transport to the active channel layer.[35] Besides, many sensing functions of OECTs require direct connection of their semiconductor channels to tissue surfaces, allowing electrostatic modulation of bulk conductivity by using biopotential or targeted biochemical signals.[108,109] The optimal interface involves direct adhesion of the semiconductor channel to the tissue surface,[110] as biological signal transduction depends on the microscale distance between the semiconducting channel and the tissue surface.[111] Gels serve as a pliable medium that facilitates the interaction between electronic devices and biological systems, enhancing contact and adhesion.[2,44]

Shiming Zhang[34] introduced an OECT-based continuous glucose monitoring (OECT-CGM) system comprising a hollow microneedle patch, an adhesive glucose oxidase (GO*x*)-loaded DN hydrogel film, and OECT glucose sensors (Fig. 5A(i and ii)). The microneedles provide a minimally invasive interface between interstitial fluid (ISF) and the OECT-CGM system. The adhesive DN hydrogel film, synthesized with an interpenetrating network (IPN) structure of PAAm and sodium alginate loaded with GO_x, serves as the gel electrolyte of the OECTs. This structure not only enhances the stability of the interface between the skin and device during movement but also facilitates the diffusion of glucose molecules from the ISF to the OECT-CGM system *via* the microneedles and hydrogel. This diffusion alters the current in the OECTs, enabling glucose monitoring (Fig. 5A(iii–vi)). Moreover, previous studies have leveraged the adhesive hydrogels for transferring conductive polymer films in OECT applications. This approach facilitates the transfer of conductive polymer films from rigid to flexible substrates, addressing the difficulty of directly handling conductive polymers on flexible materials.[112,113] For instance, Ali Khademhosseini[114] employed hydrogel electrolytes to facilitate the transfer of conductive polymer films from traditional rigid substrates to flexible ones (Fig. 5B). Initially, a PEDOT:PSS suspension, combined with surfactants like dodecylbenzenesulfonic acid (DBSA), was patterned on glass substrates. DBSA reduced the adhesion between the PEDOT:PSS film and the glass substrate. Given the stronger adhesion between

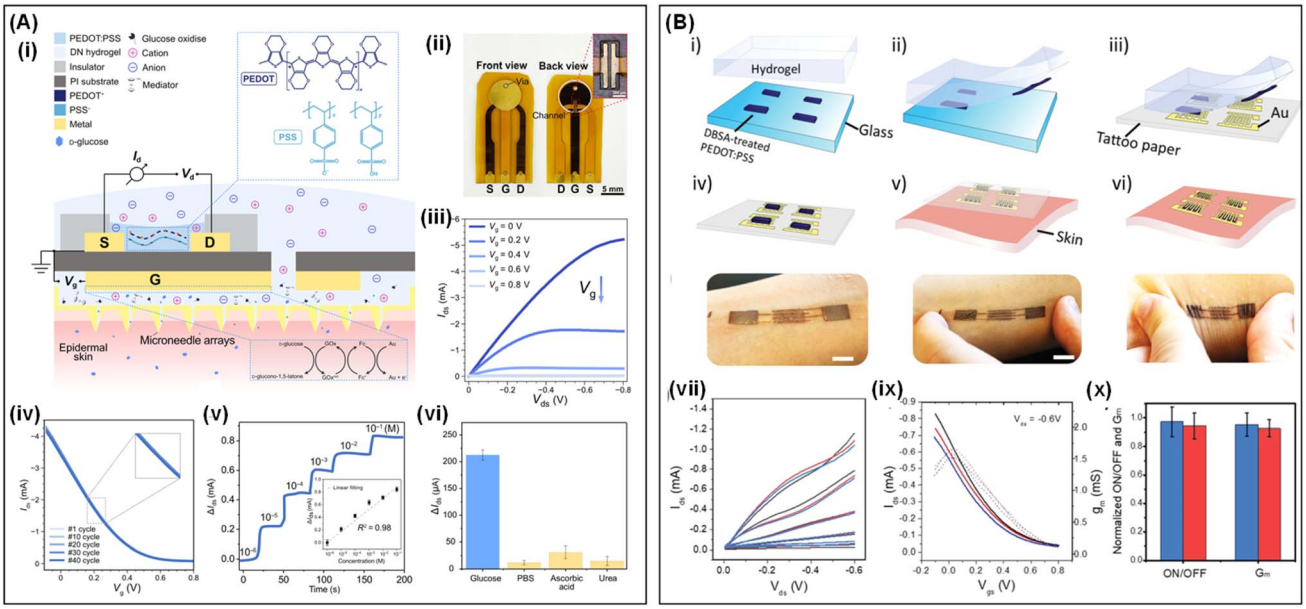

Fig. 5 (A) Fabrication and characterization of OECT-CGM. Schematic (i) and photos (ii) of the OECT-CGM and the sensing mechanism. Output curves (iii) and transfer curves (iv) of flexible OECTs. (v and vi) Response of OECT-CGM. Reproduced with permission.[34] Copyright 2024, AAAS. (B) Transfer process of PEDOT:PSS films and its soft OECT performance. (i–vi) Schematic illustration of the generic process for transferring PEDOT:PSS films with the help of hydrogel electrolyte. (vii–ix) Output and transfer curves of OECTs under released (red), 5% stretched (blue) and 40% compressed (black) conditions; (x) on/off ratio and transconductance of initial OECTs and after being compressed 10 times. Reproduced with permission.[114] Copyright 2020, Wiley-VCH.

PEDOT:PSS and the hydrogel, PEDOT:PSS could be easily transferred to various soft substrates (Fig. 5B(i–vi)). This technique enabled the creation of OECTs that are conformable and attachable to the skin, demonstrating high transconductance and a significant on/off ratio (Fig. 5B(vii–x)). These OECTs maintained stable performance even when subjected to mechanical deformation of the skin. By integrating OECTs with mobile electronic devices, a portable electronic readout system for glucose concentration monitoring was developed.

2.2.6 Stretchability. Stretchable electronic devices have garnered great attention in bioelectronics because they maintain functionality when subjected to mechanical deformation. This property is particularly valuable for applications requiring close contact with curved surfaces or sensitivity to movement, such as artificial skin, implantable electronic devices, and wearable health monitors.[115,116] Wearable electronic devices must conform to the skin and endure bending, twisting, and stretching.[117] Several studies have demonstrated that gel-based OECTs have been identified as promising candidates for stretchable bioelectronics.[118,119] The high sensitivity of stretchable OECTs in wearable and implantable biosensing and bioelectronics is crucial due to their skin-like softness and stretchability, which enable seamless integration with curved skin or tissue surfaces.[120] The stretchable solid-state OECTs enhance biocompatibility, daily usage comfort, and high-fidelity signal transduction.[121]

Sihong Wang[119] and colleagues successfully fabricated OECTs with high transconductance (223 S cm^{-1}), biaxial stretchability (100% of strain) and excellent skin compliance. This was achieved using a polymerized stretchable semiconducting polymer, poly(2-(3,3′-bis(2-(2-(2-methoxyethoxy)ethoxy)ethoxy)–[2,2′-bithiophen]-5-yl)thiophene) (p(g2T-T)), and commercially available gel electrolytes. Guoqing Zu[122] prepared stretchable OECTs using a stretchable active material and gel electrolyte. PEDOT-based aerogel films or poly(2,5-bis(3-triethyleneglycoloxythiophen-2-yl)-*co*-thiophene) (Pg2T-T)-based aerogel films, prepared *via* spin coating, sol–gel and freeze-drying protocols, served as the active layer. The polymer sol is spin-coated on a pre-stretched polyurethane (PU) to create stretchable semiconducting polymer-based aerogel films. Stretchable PAAm ion gel or ionic liquid (tris(2-hydroxyethyl)methyl ammonium methyl sulfate) was used as electrolyte (Fig. 6A(i)). This OECT exhibits a high on/off ratio, high transconductance, stretchability up to 100%, and tensile stability for 10 000 cycles at 30% strain (Fig. 6A(ii–iv)). It can also serve as a stretchable artificial synapse and biosensor for detecting dopamine (DA) (Fig. 6A(v and vi)). Fabio Cicoira[38] utilized a printed circuit board printer to fabricate fully printed and stretchable OECTs on stretchable PU (Fig. 6B(i)). To ensure overall device stretchability, printed planar gate electrodes and polyvinyl alcohol (PVA) hydrogel electrolytes were used. Flexible functionality was achieved using Ag paste for the drain, source, and gate electrodes. The PVA precursor ink was printed on the channel and gate electrodes, and crosslinked through the freeze-thawing process, *i.e.*, storing at −15 °C for 12 hours followed by thawing at room temperature. The transconductance (1.04 ± 0.13 mS) and on/off ratio (830) of resulting OECTs are comparable to those of inkjet or screen-printed OECTs (Fig. 6B(ii)). It can maintain operation for at least 50 days, with the transconductance remaining 60% of its initial value

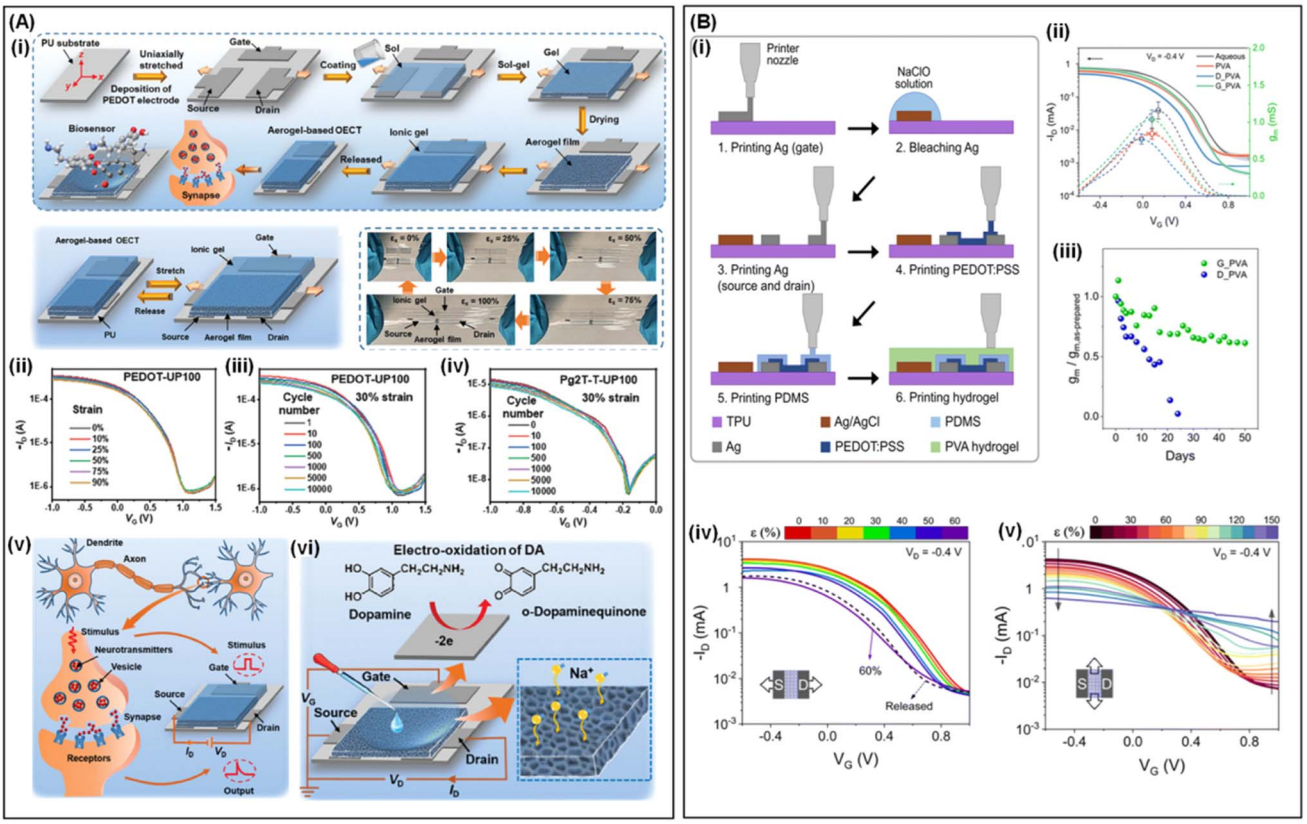

Fig. 6 (A) Fabrication and applications of semiconducting aerogel film-based OECTs. (i) The schematic illustration of a semiconducting aerogel film and stretchable OECTs. The schematic illustration of fabrication of the printed OECTs. (ii–iv) Transfer curves of OECTs based on the stretchable gel electrolyte with various tensile strains and during the stretching-releasing process for 10 000 cycles. (v and vi) The artificial synapse and biosensor of the semiconducting aerogel film-based OECTs. Reproduced with permission.[122] Copyright 2024, Wiley-VCH. (B) Preparation and characterization of printed and stretchable OECTs using PVA hydrogel electrolytes. (i) Step diagram of fabricating the printed OECTs. (ii) Transfer and transconductance curves of electrolytes. (iii) Long-term stability tests of OECTs. Transfer curves under strain in the length direction (iv) and width direction (v) of the active channel. Reproduced with permission.[38] Copyright 2023, Royal Society of Chemistry.

(Fig. 6B(iii)). Notably, the device exhibited a stretchability of 60% along the channel direction and 150% in the perpendicular direction (Fig. 6B(iv and v)), making it well-suited for the mechanical deformations encountered in wearable electronic products.

Gel electrolytes applied in OECTs offer the advantages discussed above, yet they face various challenges and drawbacks. Self-healing capability may be constrained by environmental conditions, limiting the complete restoration of mechanical and electrical properties in practical applications. High stretchability can relax the material, reducing stability and electrical conductivity. Mechanical stress during stretching may cause delamination or failure at interfaces with other materials. Responsive hydrogel electrolytes may make OECTs highly sensitive to external stimuli, potentially causing false detections or erroneous responses under non-ideal conditions like noise or environmental variations; prolonged repetitive stimuli could induce material fatigue, affecting response speed and accuracy. To maintain thermal stability, hydrogel electrolytes require compatible electrodes to prevent changes in physicochemical properties at high temperatures, potentially reducing the device lifespan. Moreover, the adhesive properties of gels are sensitive to environmental changes such as temperature and humidity, potentially affecting the reliability and accuracy of OECT sensing capabilities.

3. Application

OECTs utilizing hydrogel electrolytes provide an ideal interface with biological environments due to their inherent biocompatibility and mechanical compatibility. These devices offer local signal amplification resulting in high-fidelity sensor detection, which is crucial for bioelectronics applications. A common strategy involves modifying the gate electrode to control its electrochemical potential, thereby converting various biological signals.[123,124] Rapid cyclic voltammetry serves as a convenient characterization method for OECTs, offering speed and cost-effectiveness compared to alternative techniques.

The use of OECTs for detecting target biomarkers amidst interfering elements provides several advantages, including high selectivity, sensitivity, and low detection limits.[125] Preliminary research has highlighted the significant potential of OECTs in detecting various ions,[126–128] biomolecules (such as

enzyme,[129] cortisol,[130] immune,[131] glucose,[132,133] and metabolite[134] detection), as well as physiological signals (such as EMG[135,136] and ECG[137]). This section will delve into the exploration of solid-state OECTs based on gel electrolytes in biosensing and bioelectronics applications.

3.1 Biosensors

3.1.1 Ion sensors. Ion sensing is crucial for various applications, such as sports performance tracking, health monitoring, and clinical diagnostics. Research in ion sensing has primarily focused on three ions: K^+, Na^+, and Ca^{2+}. K^+ and Na^+ are essential for transmitting nerve impulses, muscle contraction and relaxation, and maintaining proper water balance across cell membranes.[138] Ca^{2+} is essential for building and maintaining strong bones, teeth, and nails.[139] Abnormal levels of these cations can indicate various functional disorders, including dehydration, uncontrolled diabetes, and kidney failure.[140] Changes in ion concentrations in electrolytes typically influence electrical signals of the OECTs,[141] making them valuable tools for ion sensing in healthcare and disease diagnosis.

Ion sensitive and selective OECTs have been successfully developed for various ion sensors, with notable progress in selective ion sensing applications using solid-state OECTs with hydrogel electrolytes. For instance, in 2014, Michele Sessolo[39] developed a fully solid-state OECT for K^+ selectivity utilizing a hydrogel electrolyte. The device integrates a polymer membrane allowing specific ions to pass (K^+-selective electrodes (ISM)) with the OECTs, employing a hydrogel as the electrolyte in contact with the PEDOT:PSS channel. Fig. 7A illustrates the layout of the ion-selective OECTs. The ISM is placed between the hydrogel electrolyte and the target electrolyte, isolating the channel from the gate of the OECTs. The hydrogel electrolyte, prepared by gelation at room temperature from a dispersion containing agarose, KCl, and ethylenediaminetetraacetic acid disodium salt (Na_2EDTA) as a thermal precursor, maintains K^+ selectivity.[142] A decrease in drain current proportional to K^+ concentration was observed, attributed to an increase in the number of permeating K^+ ions or a reduction in electrolyte resistance. Sensitivity to K^+ was much higher than to Na^+, confirming the membrane's ion selectivity (Fig. 7B). Additionally, the authors successfully prepared OECTs for asynchronous ion-selective sensing of other cations (K^+, Ca^{2+}, and Ag^+)[143] as well as synchronous ion-selective sensing of Ca^{2+} and NH^{4+} in sweat using different ISMs.[144] Replacing the ion solution electrolyte with a hydrogel electrolyte represents an effective approach for fabricating solid-state OECTs for multifunctional ion-selective specific sensing in the future.

3.1.2 Metabolite detection. OECTs also function as metabolite sensors, playing a critical role in clinical diagnostics and health monitoring. They detect intermediate or final products of metabolism, and changes in metabolic rates can indicate the presence of disease.[145] Metabolite sensing with OECTs can be categorized into two types: electroactive metabolites undergoing oxidation–reduction reactions on the electrode, and specific reactions of oxidoreductases with metabolite molecules. Examples of the first type include dopamine (DA),[146] ascorbic acid,[147] and uric acid (UA).[148,149] Conversely, metabolites that undergo specific reactions with oxidoreductases include glucose,[57,150,151] lactate,[152,153] cortisol,[154] as well as nucleic acids and amino acids.[155] Both types rely on changes in channel current corresponding to metabolite concentration in the electrolyte.

In recent years, solid-state OECTs based on hydrogel electrolytes have made significant progress in detecting metabolites. Researchers have achieved specific detection of metabolites through clever design of hydrogel functional groups or structures. For instance, Carlo A Bortolotti *et al.*[40] developed a flexible urea OECT-based biosensor by depositing a cross-linked gelatin hydrogel doped with urease onto a fully printed PEDOT:PSS channel material (Fig. 8A(i)). The ion substances produced by urease-catalyzed urea hydrolysis regulate the channel conductivity, enabling urea detection. A gelatin/tris hydrogel ensured the retention of protein catalytic activity and enabled selective penetration of NH_4^+ into the PEDOT:PSS channel for response specificity. This biosensor exhibited a response time of 2–3 minutes, a limit of detection of 1 μM, and a dynamic range spanning three orders of magnitude, making it suitable for urea detection in biological samples

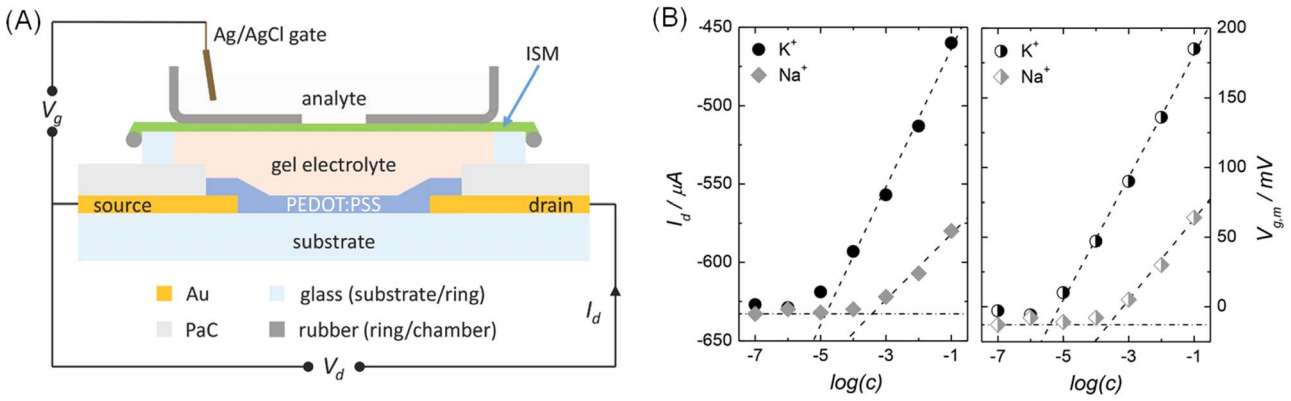

Fig. 7 (A) Schematic of K^+-selective OECTs. (B) Calibration curves of different ionic solutions obtained using K^+- selective OECTs. Reproduced with permission.[39] Copyright 2014, Wiley-VCH.

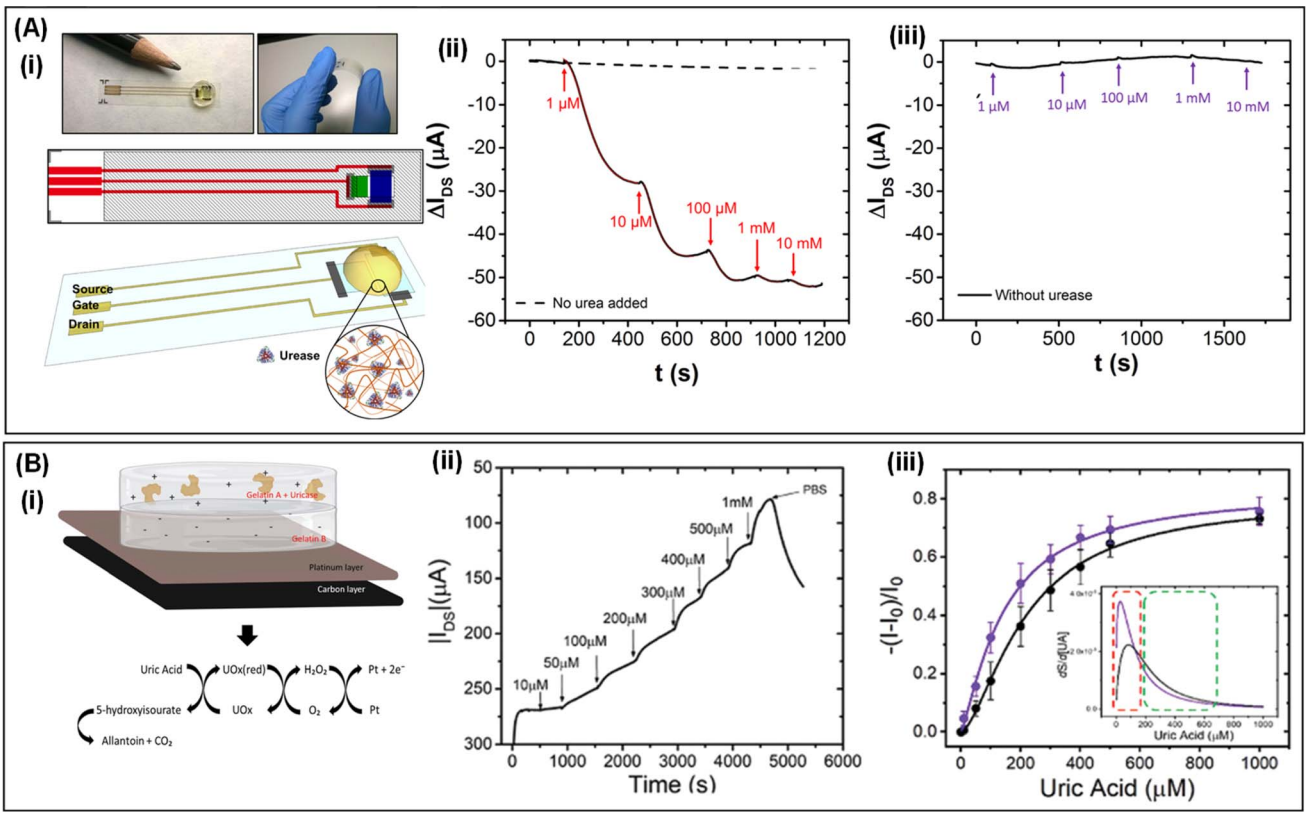

Fig. 8 (A) (i) Photographs and schematic of a flexible OECT-based biosensor for urea detection. (ii and iii) The current changes in the OECT-based urea sensor response to different concentrations of urea for a hydrogel prepared by using crosslinked urease in gelatin and controlled hydrogel without crosslinked urease. Reproduced with permission.[40] Copyright 2018, IOP publishing, Ltd (B) (i) Schematic structure of the OECT biosensor and the mechanism of UA detection. (ii and iii) The UA detection performance. (ii) Real-time drain current changes as a function of UA concentrations. (iii) Normalized current change at changing UA concentrations in PBS (black dots) and artificial wound exudate (violet dots). Reproduced with permission.[41] Copyright 2020, Wiley-VCH.

(Fig. 8A(ii and iii)). Given urea's significance in clinical analysis, especially in chronic kidney disease (CKD) monitoring, the low operating voltage (<0.5 V) of this biosensor makes it an attractive candidate for high-throughput CKD monitoring at care points or on-site.[156]

Similarly, in another study, a low-cost, disposable OECT sensor for detecting UA was developed.[41] The sensor utilized a double-layer hydrogel composed of polycationic and polyanionic gelatin with opposite charges as the electrolyte. UA detection relied on the catalytic activity of uricase (UO_x), ultimately generating H_2O_2 (Fig. 8B(i)). The double-layer hydrogel electrolyte acted as a charge-selective barrier, permitting H_2O_2 diffusion to the gate electrode for oxidation while suppressing faradaic reactions from the oxidation of electroactive molecules. Specifically, gelatin A layer consisted of a polymer network with positive charges and mobile anions to balance its charge, enhancing selectivity by hindering cation diffusion to the gate electrode. It crosslinked with UO_x, penetrating UA to react with uricase inside the gel network, catalyzing it into 5-hydroxyisourate, and ultimately converting it to allantoin spontaneously. Gelatin B, composed of a negatively charged network with mobile counterbalancing cations, prevented the diffusion of anionic electroactive substances to the gate electrode, thereby enabling a potential faradaic response. This OECT-based biosensor could operate in artificial biological fluids while maintaining sensitivity similar to that in model solutions such as PBS buffer and artificial wound exudate (Fig. 8B(ii and iii)). Elevated UA levels occur due to malnutrition,[157] metabolic disorders, or diseases such as cancer or diabetes,[158] resulting in phenomena such as urate crystal deposition in joints and kidneys and gout.[159] These examples illustrate the potential of solid-state OECTs with hydrogel electrolytes in metabolite sensing, offering promising avenues for clinical diagnostics and health monitoring.

Toshiya Sakata and colleagues[42] developed an OECT for glucose sensing utilizing a DN hydrogel. The authors synthesized the DN conductive hydrogel by polymerizing acrylamide (AAm) in a PEDOT:PSS dispersion. The first network was composed of PEDOT:PSS, while the second network was composed of PAAm incorporating sulfonic acid to improve compatibility with PEDOT and phenylboronic acid (PBA) to enhance glucose-specific affinity (Fig. 9A). This hydrogel exhibited excellent conductivity (20 S cm^{-1} in PBS) and hydration properties similar to those of soft biological tissues. By employing a simple thermal-mechanical annealing process, low-resistance contacts with gold electrodes were established.

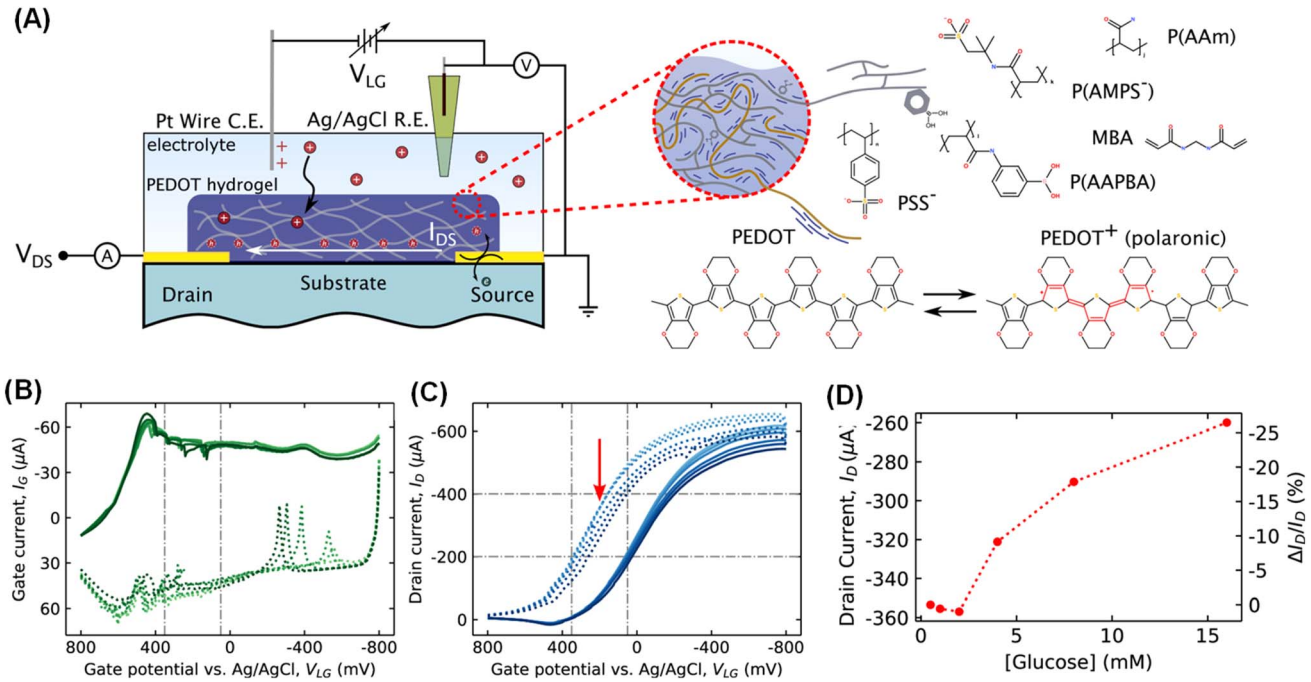

Fig. 9 (A) Schematic and mechanism of DN hydrogel-based OECTs for glucose sensing. The concurrent gate leakage (B) and transfer curves (C) during glucose sensing (darker shades and dot-dashed curves correspond to high and low glucose concentration, responsively). (D) Extracted from the midpoint potential of the ROI as indicated by the red arrow in (C). Reproduced with permission.[42] Copyright 2022, American Chemical Society.

Remarkably, the hydrogel remained stable even after continuous immersion for one month, effectively serving as the channel for OECTs. The equilibrium boronate esterification on PBA, coupled with catalytic O_2 reduction on PEDOT, enabled the direct detection and amplification of electrochemical signals originating from glucose concentrations (Fig. 9B–D). The OECTs demonstrated a transconductance of 40 mS and an on/off ratio of 10^3, allowing for linear mode operation with exceptional conductivity.

3.2 Electrophysiological signal detection

Investigating neural tissues and activities through recording and stimulation offers valuable insights into the physiological and pathological functions of the body and brain. While electrocardiography remains pivotal for capturing cardiac activity, traditional metal electrodes are not ideal for brain connectivity due to their rigidity, which leads to tissue damage and inflammation. Moreover, these electrodes are prone to noise interference from transmission lines and external circuits, reducing their effectiveness. Achieving high-quality electroencephalogram (EEG) and electrocardiography (ECG) signals often requires strong chemical adhesives to bond electrodes to the scalp surface or intracranially, potentially causing tissue damage and immune system reactions in the brain.[13,160] Soft and flexible materials utilized in OECTs offer a promising solution by directly amplifying input signals recorded from the site, making them ideal for measuring electrophysiological signals. To ensure stable and long-term measurements, hydrogels or IL gels are used to improve interaction between electronic devices and the skin, thereby providing valuable techniques for study and diagnosis of brain-related diseases.

Khodagholy and colleagues[43] devised flexible, biocompatible, internal ion-gated OECTs that feature high transconductance, rapid response time, and great conformability to amplify and record high-quality neural physiological activities (EEG) in the brain (Fig. 10A(i)). This device uses a conductive polymer PEDOT:PSS, combined with D-sorbitol to form an ionic reservoir, which facilitates ion transport channels and enhances the conductivity of PEDOT:PSS. A chitosan hydrogel serves as an ion membrane between the gate and channel, offering biocompatibility, stability, and solution processability. This minimizes electrochemical impedance at the skin–electrode interface, thus reducing skin redness or irritation. This OECT successfully captured clear neural oscillations at approximately 8–12 Hz (α) from the occipital area during quiet wakefulness with eyes closed, consistent with a posterior-dominant rhythm (Fig. 10A(ii)). It also recorded higher-frequency brain oscillations occurring simultaneously at (13–25 Hz, β) and (30–50 Hz, γ), highlighting the OECT's capability to perform various neural computations and information transmission between cortical areas.

Sahika Inal *et al.*[53] developed three types of gel electrolytes with the same polymer matrices but different ionic components: saline solutions, ILs, and deep eutectic solvents (DESs). These electrolytes were evaluated for their performance in OECTs to study the influence of electrolyte types on OECT properties (Fig. 10B(i)). The DES electrolyte, prepared with poly (diglycidyl ether of bisphenol-A) (DGLY) as the polymer matrix

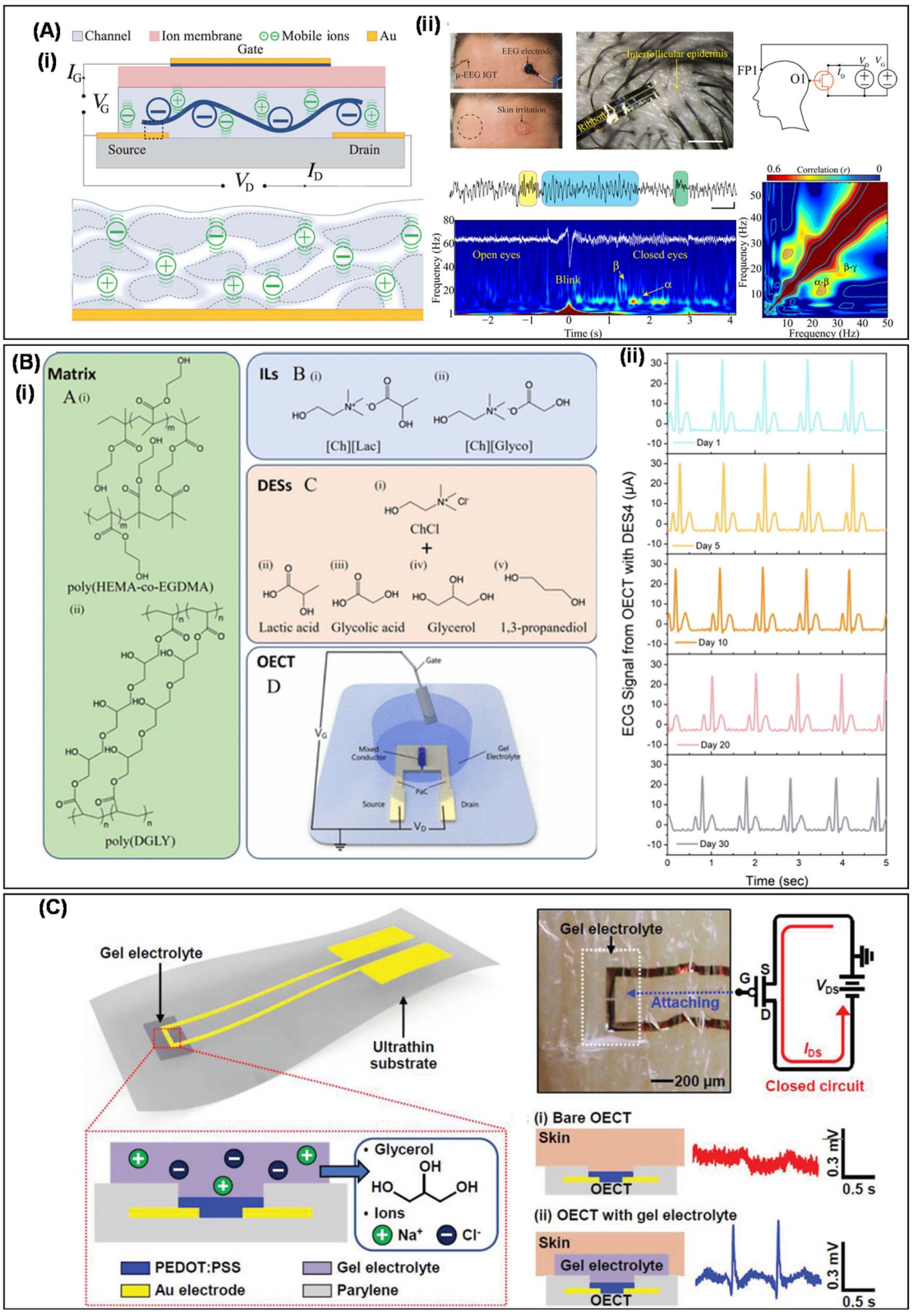

Fig. 10 (A) (i) Schematic illustration of OECTs and (ii) recording of EEG signals by OECTs that are attached on the human scalp during opening and closing of the eyes. Reproduced with permission.[43] Copyright 2019, AAAS. (B) (i) Chemical structures of the gel electrolyte and the OECT architecture. (ii) ECG acquisition with the best eutectogel-gated OECTs. Reproduced with permission.[53] CC BY 4.0. (C) Architecture of an ultrathin wearable OECT with nonvolatile gel electrolyte and its application in ECG measurement from the skin. Reproduced with permission.[44] Copyright 2019, Wiley-VCH.

Table 1 Comparison of current solid-state OECTs based on gel electrolytes

Gel electrolyte	Gelation method	Properties and functions	Main parameters	Application	Ref.
PVA	Freezing–thawing	Self-healing	Self-healing ratio: 85–100%	Ion sensor (detect Na^+)	35
Gelatin	Heating–cooling	pH-responsive	V_{out} and gain range from 1.1 to 0.46 V and 1.92 to 0.63 at pH = 1.13–13.43	Electrochemical logic circuits (NOT, NOR, and NAND gates)	37
PVA-PAAm	Photolithography and photo polymerization	Flexible and nonvolatile	>8 days stability	ECG monitoring	44
IL gel composite of PVDF-*co*-HFP and EMIM BF4	Spin-coating	Wide temperature-resistance	Transient speed values are ≈0.1 ms at 25 °C and ≈1.9 ms at −40 °C	ECG monitoring	78
DN hydrogel (PAAm/carrageenan)	Thermal polymerization	Temperature-resistance	> 4 months stability; operation at −30 °C ∼20 °C	Mimic synaptic functions	36
DN hydrogel (PAAm/carrageenan)	Thermal polymerization	Temperature-resistance	Operation at −30 °C ∼20 °C	Ion sensor (detect various [KCl])	58
DN hydrogel (PAAm/Na^+-alginate/GO*x*)	Photo polymerization	Adhesion	Great SNR: ∼60 dB	Glucose monitoring	34
PVA/gelatin; PVA/agarose	Heating–cooling	Adhesion	Enable transfer-printing of PEDOT:PSS films; transconductance: ∼1.5 mS; on/off: ∼50	Glucose monitoring	114
Commercial gel (Bio-Protech, T716-50)	—	Stretchability	Transconductance: ≈223 S cm^{-1}; biaxial stretchability: 100% strain	ECG monitoring	119
PAAm ion gel or ionic liquid (tris(2-hydroxyethyl)methyl ammonium methyl sulfate)	Photo polymerization	Stretchability	High on/off ratio; stretchability: 100% strain; tensile stability: 10 000 cycles at 30% strain	DA detection	122
PVA; Glycerol-PVA; DMSO-PVA	Freezing–thawing	Stretchability	Transconductance: 1.04 ± 0.13 mS; on/off ratio: 830; stretchability: channel direction of ∼60% strain and perpendicular direction of 150% strain	—	38
Agarose/Na_2EDTA/KCl	Heating–cooling	K^+ selectivity	High selectivity coefficient (−log K_{K^+}, Na^+: 2.7)	Ion sensor (detect K^+)	39
Gelatin/tris	Cooling	Ensure the retention of protein catalytic activity and enable selective penetration of NH_4^+	Low LODs: 1 μM; response time: 2–3 min	Urea detection	40
Double-layer opposite-charged hydrogel (polycations and polyanions gelatin)	Crosslinked by glutaraldehyde	Function as a charge-selective barrier	Low LODs [UA]: 4.5×10^{-6} M	UA detection	41
DN hydrogel (PEDOT:PSS/PAAm-PAMPS-PBA)	Thermal polymerization	Glucose specific	Transconductance: 40 mS; on/off ratio: 10^3	Glucose detection	42
Chitosan	Spin-coating	Acting as an ion membrane	Transconductance: 32.30 mS; >100 days stability	EEG monitoring	43
Poly(HEMA-*co*-EGDMA) and poly(DGLY) with three different ionic components (saline solutions, ILs, and deep eutectic solvents (DESs))	Photo polymerization	Construction of p-type depletion and p-type and n-type enhancement mode devices	Transconductance: ∼27 mS; on/off ratio: 4.0×10^5; switching speed: 24 ms	ECG monitoring	53
PVA/PAAm with glycerol-ionic solution	Photolithography and photo polymerization	Anti-drying and long term stability	Transconductance: 1.62 mS; > 8 days stability	ECG monitoring	44
P(VDF-HFP) with [EMI][TFSI]	Drop-casting	Realizing a fully printed OECT	Transconductance: 1.1 mS	—	161

and choline chloride (ChCl) with 1,3-propanediol as the ionic component, outperformed the other two gel electrolytes, in p-type depletion-mode and p-type and n-type enhancement-mode OECTs. This OECT demonstrated excellent stability in long-term ECG signal monitoring, maintaining a consistent signal-to-noise ratio (SNR) even after 5 hours and 30 days of continuous operation (Fig. 10B(ii)). Takao Someya *et al.*[44] reported ultra-thin wearable OECTs for detecting ECG signals based on non-volatile hydrogel electrolytes, capable of operating on dry biological surfaces. The gel electrolyte consists of a dispersed phase of glycerol-ionic solution and a matrix of PVA and PAAm (Fig. 10C(i)). The low volatility of glycerol ensures stability and anti-drying properties. The gel also maintains good mechanical stability under physical deformation. Moreover, the developed OECTs can uniformly adhere to the skin, effectively monitoring cardiac signals from the skin continuously for long-term applications (Fig. 10C(ii)), thus overcoming the contact limitations of previous OECTs.

The current existing solid-state OECTs based on gel electrolytes and their performance are listed and compared in Table 1. The development of solid-state OECTs has progressed from incorporating soft gel electrolytes with various properties to creating high-performance OECTs, and finally to integrating these devices into wearable or implantable biosensors and bioelectronics.

4. Challenges and perspectives

In this comprehensive review, we systematically present the latest advancements in solid-state OECTs based on gel electrolytes, encompassing the classification and properties of gel electrolytes. The prolific research conducted on the OECT underscores the persisting demand for their widespread applications. As elucidated, OECTs employing gel electrolytes hold promise in various fields such as ion sensors, biosensors, and electrophysiological monitoring devices. Despite significant efforts directed towards exploring novel bioelectronic applications leveraging gel electrolytes for solid-state OECTs, several challenges remain to be addressed and improved upon.

In terms of manufacturing techniques, traditional OECT device fabrication involves simple processes like inkjet printing[162] and screen printing,[28] offering unique advantages for producing low-cost and large-area electronic devices. However, the current approach of manually applying hydrogel electrolytes to OECT devices constrains their scalability. Although previous work has combined water-based inkjet-printed PEDOT:PSS electrodes and solution-processable ionic gel dielectrics to achieve fully printed OECTs in environmentally friendly solvents,[161] more work should systematically explore and design hydrogel precursor solutions with tailored viscosities suitable for various printing processes (*e.g.*, low viscosity for inkjet printers and high viscosity for screen printers), by studying relevant standard parameters, thereby facilitating their integration into solid-state OECTs through printing processes.

Smart solid-state OECTs incorporating responsive hydrogel electrolytes are still at nascent stages. Although some examples exist of using acid- and alkali-modified gelatin to prepare electrolytes capable of regulating channel conductivity by modulating the concentration of H^+ and OH^- at the electrolyte–channel interface,[37] the development of responsive OECTs remains relatively limited. Future endeavors could harness the multi-responsiveness of hydrogel electrolytes (*e.g.*, to ions, temperature, light, electric field, magnetic field, *etc.*) to design more intelligent solid-state OECT sensors or bioelectronic devices, thereby broadening their application scenarios. Particularly, integrating drug-controllable loading and release mechanisms into responsive gels could confer dual-functionality for diagnosing and treating diseases using solid-state OECTs. Moreover, by judiciously incorporating various endogenous (chemical and biological) and exogenous (physical) stimuli-responsive units into hydrogel systems, a versatile "toolbox" can be devised to tailor smart OECTs, representing an effective approach for programming or integrating diverse functional OECTs. Additionally, employing biodegradable hydrogels can propel the development of implantable devices for recording or stimulating electrogenic cells.

The pursuit of high-density and implantable biochips for real-time health monitoring necessitates self-powered operation, wireless communication, and low-power functionalities. To fulfill these requirements, energy storage devices based on hydrogel electrolytes have been extensively researched,[163,164] including freeze-resistant batteries capable of operating safely at low temperatures,[165] stretchable flexible capacitors[166] and batteries,[167,168] and long-lasting batteries.[169] Integrating solid-state OECTs based on hydrogel electrolytes with hydrogel batteries holds promise for fully flexible, self-powered, and biocompatible solid-state sensors. Moreover, the realization of wireless signal transmission and noise suppression functionalities is anticipated through the integration of OECT technology and the continuous advancement of current digital circuits.

Conflicts of interest

There are no conflicts to declare.

Acknowledgements

This work was supported by the Shenzhen Fundamental Research Funding (JCYJ20220530113802006), the Guangdong Basic and Applied Basic Research Foundation (2023A1515110012), the National Natural Science Foundation of China (22405030 and 22305047), the Dongguan Science and Technology of Social Development Program (20231800939852), the Guangdong Basic and Applied Basic Research Foundation (2023A1515140114), and the open research fund of Songshan Lake Materials Laboratory (2022SLABFN06).

References

1 J. Rivnay, S. Inal, A. Salleo, R. M. Owens, M. Berggren and G. G. Malliaras, Organic electrochemical transistors, *Nat. Rev. Mater.*, 2018, **3**(2), 1–14.
2 T. Someya, Z. Bao and G. G. Malliaras, The rise of plastic bioelectronics, *Nature*, 2016, **540**(7633), 379–385.

3 Y. Niu, Z. Qin, Y. Zhang, C. Chen, S. Liu and H. Chen, Expanding the potential of biosensors: a review on organic field effect transistor (OFET) and organic electrochemical transistor (OECT) biosensors, *Mater. Futures*, 2023, **2**(4), 042401.
4 W. Huang, J. Chen, Y. Yao, D. Zheng, X. Ji, L.-W. Feng, D. Moore, N. R. Glavin, M. Xie and Y. Chen, Vertical organic electrochemical transistors for complementary circuits, *Nature*, 2023, **613**(7944), 496–502.
5 P. Lin, F. Yan and H. L. Chan, Ion-sensitive properties of organic electrochemical transistors, *ACS Appl. Mater. Interfaces*, 2010, **2**(6), 1637–1641.
6 Y. Kim, T. Lim, C.-H. Kim, C. S. Yeo, K. Seo, S.-M. Kim, J. Kim, S. Y. Park, S. Ju and M.-H. Yoon, Organic electrochemical transistor-based channel dimension-independent single-strand wearable sweat sensors, *NPG Asia Mater.*, 2018, **10**(11), 1086–1095.
7 W. Tao, P. Lin, J. Hu, S. Ke, J. Song and X. Zeng, A sensitive DNA sensor based on an organic electrochemical transistor using a peptide nucleic acid-modified nanoporous gold gate electrode, *RSC Adv.*, 2017, **7**(82), 52118–52124.
8 E. Bihar, Y. Deng, T. Miyake, M. Saadaoui, G. G. Malliaras and M. Rolandi, A disposable paper breathalyzer with an alcohol sensing organic electrochemical transistor, *Sci. Rep.*, 2016, **6**(1), 27582.
9 H. Tang, F. Yan, P. Lin, J. Xu and H. L. Chan, Highly sensitive glucose biosensors based on organic electrochemical transistors using platinum gate electrodes modified with enzyme and nanomaterials, *Adv. Funct. Mater.*, 2011, **21**(12), 2264–2272.
10 J. Rivnay, M. Ramuz, P. Leleux, A. Hama, M. Huerta and R. M. Owens, Organic electrochemical transistors for cell-based impedance sensing, *Appl. Phys. Lett.*, 2015, **106**(4), 043301.
11 P. Lin, F. Yan, J. Yu, H. L. Chan and M. Yang, The application of organic electrochemical transistors in cell-based biosensors, *Adv. Mater.*, 2010, **33**(22), 3655–3660.
12 H. S. White, G. P. Kittlesen and M. S. Wrighton, Chemical derivatization of an array of three gold microelectrodes with polypyrrole: fabrication of a molecule-based transistor, *J. Am. Chem. Soc.*, 1984, **106**(18), 5375–5377.
13 J. Rivnay, P. Leleux, M. Ferro, M. Sessolo, A. Williamson, D. A. Koutsouras, D. Khodagholy, M. Ramuz, X. Strakosas and R. M. Owens, High-performance transistors for bioelectronics through tuning of channel thickness, *Sci. Adv.*, 2015, **1**(4), e1400251.
14 X. Wu, A. Surendran, J. Ko, O. Filonik, E. M. Herzig, P. Müller-Buschbaum and W. L. Leong, Ionic-liquid doping enables high transconductance, fast response time, and high ion sensitivity in organic electrochemical transistors, *Adv. Mater.*, 2019, **31**(2), 1805544.
15 W. Wu, K. Feng, Y. Wang, J. Wang, E. Huang, Y. Li, S. Y. Jeong, H. Y. Woo, K. Yang and X. Guo, Selenophene Substitution Enabled High-Performance n-Type Polymeric Mixed Ionic-Electronic Conductors for Organic Electrochemical Transistors and Glucose Sensors, *Adv. Mater.*, 2024, **36**(1), 2310503.
16 K. Feng, W. Shan, J. Wang, J. W. Lee, W. Yang, W. Wu, Y. Wang, B. J. Kim, X. Guo and H. Guo, Cyano-Functionalized n-Type Polymer with High Electron Mobility for High-Performance Organic Electrochemical Transistors, *Adv. Mater.*, 2022, **34**(24), 2201340.
17 Y. Kim, H. Noh, B. D. Paulsen, J. Kim, I. Y. Jo, H. Ahn, J. Rivnay and M. H. Yoon, Strain-engineering induced anisotropic crystallite orientation and maximized carrier mobility for high-performance microfiber-based organic bioelectronic devices, *Adv. Mater.*, 2021, **33**(10), 2007550.
18 S.-M. Kim, C.-H. Kim, Y. Kim, N. Kim, W.-J. Lee, E.-H. Lee, D. Kim, S. Park, K. Lee and J. Rivnay, Influence of PEDOT: PSS crystallinity and composition on electrochemical transistor performance and long-term stability, *Nat. Commun.*, 2018, **9**(1), 3858.
19 A. Savva, R. Hallani, C. Cendra, J. Surgailis, T. C. Hidalgo, S. Wustoni, R. Sheelamanthula, X. Chen, M. Kirkus and A. Giovannitti, Balancing ionic and electronic conduction for high-performance organic electrochemical transistors, *Adv. Funct. Mater.*, 2020, **30**(11), 1907657.
20 C. Pitsalidis, A. M. Pappa, M. Porel, C. M. Artim, G. C. Faria, D. D. Duong, C. A. Alabi, S. Daniel, A. Salleo and R. M. Owens, Biomimetic electronic devices for measuring bacterial membrane disruption, *Adv. Mater.*, 2018, **30**(39), 1803130.
21 P. C. Hütter, T. Rothländer, A. Haase, G. Trimmel and B. Stadlober, Influence of geometry variations on the response of organic electrochemical transistors, *Appl. Phys. Lett.*, 2013, **103**(4), 043308.
22 D. A. Bernards and G. G. Malliaras, Steady-state and transient behavior of organic electrochemical transistors, *Adv. Funct. Mater.*, 2007, **17**(17), 3538–3544.
23 S. Inal, G. G. Malliaras and J. Rivnay, Benchmarking organic mixed conductors for transistors, *Nat. Commun.*, 2017, **8**(1), 1767.
24 C. M. Proctor, J. Rivnay and G. G. Malliaras, Understanding volumetric capacitance in conducting polymers, *J. Polym. Sci., Part B: Polym. Phys.*, 2016, **54**, 1433–1436.
25 Y. Li, S. Zhang, X. Li, V. R. N. Unnava and F. Cicoira, Highly stretchable PEDOT: PSS organic electrochemical transistors achieved via polyethylene glycol addition, *Flex. Print. Electron.*, 2019, **4**(4), 044004.
26 S. Dai, Y. Dai, Z. Zhao, F. Xia, Y. Li, Y. Liu, P. Cheng, J. Strzalka, S. Li and N. Li, Intrinsically stretchable neuromorphic devices for on-body processing of health data with artificial intelligence, *Matter*, 2022, **5**(10), 3375–3390.
27 O. Parlak, S. T. Keene, A. Marais, V. F. Curto and A. Salleo, Molecularly selective nanoporous membrane-based wearable organic electrochemical device for noninvasive cortisol sensing, *Sci. Adv.*, 2018, **4**(7), eaar2904.
28 P. Andersson Ersman, R. Lassnig, J. Strandberg, D. Tu, V. Keshmiri, R. Forchheimer, S. Fabiano, G. Gustafsson and M. Berggren, All-printed large-scale integrated circuits based on organic electrochemical transistors, *Nat. Commun.*, 2019, **10**(1), 5053.

29 L. V. Kayser and D. J. Lipomi, Stretchable conductive polymers and composites based on PEDOT and PEDOT:PSS, *Adv. Mater.*, 2019, **31**(10), 1806133.
30 I. Gualandi, M. Marzocchi, A. Achilli, D. Cavedale, A. Bonfiglio and B. Fraboni, Textile organic electrochemical transistors as a platform for wearable biosensors, *Sci. Rep.*, 2016, **6**(1), 33637.
31 A. K. Means and M. A. Grunlan, Modern strategies to achieve tissue-mimetic, mechanically robust hydrogels, *ACS Macro Lett.*, 2019, **8**, 705–713.
32 H. Yuk, B. Lu and X. Zhao, Hydrogel bioelectronics, *Chem. Soc. Rev.*, 2019, **48**(6), 1642–1667.
33 X. Liu, J. Liu, S. Lin and X. Zhao, Hydrogel machines, *Mater. Today*, 2020, **36**, 102–124.
34 J. Bai, D. Liu, X. Tian, Y. Wang, B. Cui, Y. Yang, S. Dai, W. Lin, J. Zhu, J. Wang, A. Xu, Z. Gu and S. Zhang, Coin-sized, fully integrated, and minimally invasive continuous glucose monitoring system based on organic electrochemical transistors, *Sci. Adv.*, 2024, **10**(16), eadl1856.
35 J. Ko, X. Wu, A. Surendran, B. T. Muhammad and W. L. Leong, Self-healable organic electrochemical transistor with high transconductance, fast response, and long-term stability, *ACS Appl. Mater. Interfaces*, 2020, **12**(30), 33979–33988.
36 S. Han, S. Yu, S. Hu, H.-j. Chen, J. Wu and C. Liu, A high endurance, temperature-resilient, and robust organic electrochemical transistor for neuromorphic circuits, *J. Mater. Chem. C*, 2021, **9**(35), 11801–11808.
37 Y. J. Jo, K. Y. Kwon, Z. U. Khan, X. Crispin and T.-i. Kim, Gelatin hydrogel-based organic electrochemical transistors and their integrated logic circuits, *ACS Appl. Mater. Interfaces*, 2018, **10**(45), 39083–39090.
38 C.-H. Kim, M. Azimi, J. Fan, H. Nagarajan, M. Wang and F. Cicoira, All-printed and stretchable organic electrochemical transistors using a hydrogel electrolyte, *Nanoscale*, 2023, **15**(7), 3263–3272.
39 M. Sessolo, J. Rivnay, E. Bandiello, G. G. Malliaras and H. J. Bolink, Ion-selective organic electrochemical transistors, *Adv. Mater.*, 2014, **26**(28), 4803–4807.
40 M. Berto, C. Diacci, L. Theuer, M. Di Lauro, D. T. Simon, M. Berggren, F. Biscarini, V. Beni and C. A. Bortolotti, Label free urea biosensor based on organic electrochemical transistors, *Flex. Print. Electron.*, 2018, **3**(2), 024001.
41 M. Galliani, C. Diacci, M. Berto, M. Sensi, V. Beni, M. Berggren, M. Borsari, D. T. Simon, F. Biscarini and C. A. Bortolotti, Flexible printed organic electrochemical transistors for the detection of uric acid in artificial wound exudate, *Adv. Mater. Interfaces*, 2020, **7**(23), 2001218.
42 A. C. Tseng and T. Sakata, Direct electrochemical signaling in organic electrochemical transistors comprising high-conductivity double-network hydrogels, *ACS Appl. Mater. Interfaces*, 2022, **14**(21), 24729–24740.
43 G. D. Spyropoulos, J. N. Gelinas and D. Khodagholy, Internal ion-gated organic electrochemical transistor: A building block for integrated bioelectronics, *Sci. Adv.*, 2019, **5**(2), eaau7378.
44 H. Lee, S. Lee, W. Lee, T. Yokota, K. Fukuda and T. Someya, Ultrathin organic electrochemical transistor with nonvolatile and thin gel electrolyte for long-term electrophysiological monitoring, *Adv. Funct. Mater.*, 2019, **29**(48), 1906982.
45 S. Correa, A. K. Grosskopf, H. Lopez Hernandez, D. Chan, A. C. Yu, L. M. Stapleton and E. A. Appel, Translational applications of hydrogels, *Chem. Rev.*, 2021, **121**(18), 11385–11457.
46 R. Borem, A. Madeline, J. Walters, H. Mayo, S. Gill and J. Mercuri, Angle-ply biomaterial scaffold for annulus fibrosus repair replicates native tissue mechanical properties, restores spinal kinematics, and supports cell viability, *Acta Biomater.*, 2017, **58**, 254–268.
47 Y. Zeng, C. Chen, W. Liu, Q. Fu, Z. Han, Y. Li, S. Feng, X. Li, C. Qi and J. Wu, Injectable microcryogels reinforced alginate encapsulation of mesenchymal stromal cells for leak-proof delivery and alleviation of canine disc degeneration, *Biomaterials*, 2015, **59**, 53–65.
48 H. Yuk, J. Wu and X. Zhao, Hydrogel interfaces for merging humans and machines, *Nat. Rev. Mater.*, 2022, **7**(12), 935–952.
49 Y.-T. Kim, Y.-S. Hong, R. M. Kimmel, J.-H. Rho and C.-H. Lee, New approach for characterization of gelatin biopolymer films using proton behavior determined by low field 1H NMR spectrometry, *J. Agric. Food Chem.*, 2007, **55**(26), 10678–10684.
50 M. Silva, P. Barbosa, L. Rodrigues, A. Gonçalves, C. Costa and E. Fortunato, Gelatin in electrochromic devices, *Opt. Mater.*, 2010, **32**(6), 719–722.
51 T. Basu, T. Middya and S. Tarafdar, Ion-conductivity study and anomalous diffusion analysis of plasticized gelatin films, *J. Appl. Polym. Sci.*, 2013, **130**(4), 3018–3024.
52 T. Nguyen-Dang, K. Harrison, A. Lill, A. Dixon, E. Lewis, J. Vollbrecht, T. Hachisu, S. Biswas, Y. Visell and T. Q. Nguyen, Biomaterial-Based Solid-Electrolyte Organic Electrochemical Transistors for Electronic and Neuromorphic Applications, *Adv. Electron. Mater.*, 2021, **7**(12), 2100519.
53 Y. Zhong, N. Lopez-Larrea, M. Alvarez-Tirado, N. Casado, A. Koklu, A. Marks, M. Moser, I. McCulloch, D. Mecerreyes and S. Inal, Eutectogels as a Semisolid Electrolyte for Organic Electrochemical Transistors, *Chem. Mater.*, 2024, **36**, 1841–1854.
54 I. Del Agua, L. Porcarelli, V. Curto, A. Sanchez-Sanchez, E. Ismailova, G. Malliaras and D. Mecerreyes, A Na+ conducting hydrogel for protection of organic electrochemical transistors, *J. Mater. Chem. B*, 2018, **6**(18), 2901–2906.
55 D. Khodagholy, V. F. Curto, K. J. Fraser, M. Gurfinkel, R. Byrne, D. Diamond, G. G. Malliaras, F. Benito-Lopez and R. M. Owens, Organic electrochemical transistor incorporating an ionogel as a solid state electrolyte for lactate sensing, *J. Mater. Chem.*, 2012, **22**(10), 4440–4443.

56 C. P. Tseng, F. Liu, X. Zhang, P. C. Huang, I. Campbell, Y. Li, J. T. Atkinson, T. Terlier, C. M. Ajo-Franklin and J. J. Silberg, Solution-deposited and Patternable conductive polymer thin-film electrodes for microbial bioelectronics, *Adv. Mater.*, 2022, **34**(13), 2109442.

57 M. E. Welch, T. Doublet, C. Bernard, G. G. Malliaras and C. K. Ober, A glucose sensor via stable immobilization of the GOx enzyme on an organic transistor using a polymer brush, *J. Polym. Sci., Part A: Polym. Chem.*, 2015, **53**(2), 372–377.

58 S. Han, S. Yu, S. Hu, X. Liang, Y. Luo and C. Liu, Ion transport to temperature and gate in organic electrochemical transistors with anti-freezing hydrogel, *Org. Electron.*, 2022, **108**, 106605.

59 L. Zhang, D. Jiang, T. Dong, R. Das, D. Pan, C. Sun, Z. Wu, Q. Zhang, C. Liu and Z. Guo, Overview of ionogels in flexible electronics, *Chem. Rec.*, 2020, **20**(9), 948–967.

60 F. Ghorbanizamani, H. Moulahoum, E. G. Celik and S. Timur, Ionic liquids enhancement of hydrogels and impact on biosensing applications, *J. Mol. Liq.*, 2022, **357**, 119075.

61 X. Wang and J. Hao, Recent advances in ionic liquid-based electrochemical biosensors, *Sci. Bull.*, 2016, **61**(16), 1281–1295.

62 D. Wang, S. Zhao, R. Yin, L. Li, Z. Lou and G. Shen, Recent advanced applications of ion-gel in ionic-gated transistor, *npj Flexible Electron.*, 2021, **5**(1), 13.

63 N. Gao, X. Wu, Y. He, Q. Ma and Y. Wang, Reconfigurable and recyclable circuits based on liquid passive components, *Adv. Electron. Mater.*, 2020, **6**(8), 1901388.

64 R. He, A. Lv, X. Jiang, C. Cai, Y. Wang, W. Yue, L. Huang, X. B. Yin and L. Chi, Organic Electrochemical Transistor Based on Hydrophobic Polymer Tuned by Ionic Gels, *Angew. Chem., Int. Ed.*, 2023, **62**(37), e202304549.

65 V. Amoli, J. S. Kim, S. Y. Kim, J. Koo, Y. S. Chung, H. Choi and D. H. Kim, Ionic tactile sensors for emerging human-interactive technologies: a review of recent progress, *Adv. Funct. Mater.*, 2020, **30**(20), 1904532.

66 R. Li, L. Wang, D. Kong and L. Yin, Recent progress on biodegradable materials and transient electronics, *Bioact. Mater.*, 2018, **3**(3), 322–333.

67 Y. Zhao, S. Haseena, M. K. Ravva, S. Zhang, X. Li, J. Jiang, Y. Fu, S. Inal, Q. Wang and Y. Wang, Side chain engineering enhances the high-temperature resilience and ambient stability of organic synaptic transistors for neuromorphic applications, *Nano Energy*, 2022, **104**, 107985.

68 G. C. Luque, M. L. Picchio, A. P. Martins, A. Dominguez-Alfaro, N. Ramos, I. del Agua, B. Marchiori, D. Mecerreyes, R. J. Minari and L. C. Tomé, 3D printable and biocompatible iongels for body sensor applications, *Adv. Electron. Mater.*, 2021, **7**(8), 2100178.

69 M. Isik, T. Lonjaret, H. Sardon, R. Marcilla, T. Herve, G. G. Malliaras, E. Ismailova and D. Mecerreyes, Cholinium-based ion gels as solid electrolytes for long-term cutaneous electrophysiology, *J. Mater. Chem. C*, 2015, **3**(34), 8942–8948.

70 H. Wang, Z. Wang, J. Yang, C. Xu, Q. Zhang and Z. Peng, Ionic gels and their applications in stretchable electronics, *Macromol. Rapid Commun.*, 2018, **39**(16), 1800246.

71 T. P. Lodge and T. Ueki, Mechanically tunable, readily processable ion gels by self-assembly of block copolymers in ionic liquids, *Acc. Chem. Res.*, 2016, **49**(10), 2107–2114.

72 Y. Hong, Z. Lin, Y. Yang, T. Jiang, J. Shang and Z. Luo, Biocompatible conductive hydrogels: applications in the field of biomedicine, *Int. J. Mol. Sci.*, 2022, **23**(9), 4578.

73 F. Zhao, Y. Shi, L. Pan and G. Yu, Multifunctional nanostructured conductive polymer gels: synthesis, properties, and applications, *Acc. Chem. Res.*, 2017, **50**(7), 1734–1743.

74 Y. Wang, C. Zhu, R. Pfattner, H. Yan, L. Jin, S. Chen, F. Molina-Lopez, F. Lissel, J. Liu and N. I. Rabiah, A highly stretchable, transparent, and conductive polymer, *Sci. Adv.*, 2017, **3**(3), e1602076.

75 A. Nawaz, Q. Liu, W. L. Leong, K. E. Fairfull-Smith and P. Sonar, Organic electrochemical transistors for in vivo bioelectronics, *Adv. Mater.*, 2021, **33**(49), 2101874.

76 S. Inal, J. Rivnay, A.-O. Suiu, G. G. Malliaras and I. McCulloch, Conjugated polymers in bioelectronics, *Acc. Chem. Res.*, 2018, **51**(6), 1368–1376.

77 A. Kavanagh, R. Byrne, D. Diamond and K. J. Fraser, Stimuli responsive ionogels for sensing applications—an overview, *Membranes*, 2012, **2**(1), 16–39.

78 X. Wu, S. Chen, M. Moser, A. Moudgil, S. Griggs, A. Marks, T. Li, I. McCulloch and W. L. Leong, High Performing Solid-State Organic Electrochemical Transistors Enabled by Glycolated Polythiophene and Ion-Gel Electrolyte with a Wide Operation Temperature Range from− 50 to 110 ° C, *Adv. Funct. Mater.*, 2023, **33**(3), 2209354.

79 S. Zhang and F. Cicoira, Water-enabled healing of conducting polymer films, *Adv. Mater.*, 2017, **29**(40), 1703098.

80 M. M. Perera and N. Ayres, Dynamic covalent bonds in self-healing, shape memory, and controllable stiffness hydrogels, *Polym. Chem.*, 2020, **11**(8), 1410–1423.

81 Z. Gong, G. Zhang, X. Zeng, J. Li, G. Li, W. Huang, R. Sun and C. Wong, High-strength, tough, fatigue resistant, and self-healing hydrogel based on dual physically cross-linked network, *ACS Appl. Mater. Interfaces*, 2016, **8**(36), 24030–24037.

82 C. Cai, X. Zhang, Y. Li, X. Liu, S. Wang, M. Lu, X. Yan, L. Deng, S. Liu and F. Wang, Self-healing hydrogel embodied with macrophage-regulation and responsive-gene-silencing properties for synergistic prevention of peritendinous adhesion, *Adv. Mater.*, 2022, **34**(5), 2106564.

83 Z. Zhu, D. Lu, M. Zhu, P. Zhang and X. Xiang, Smart Organogels with Antiswelling, Strong Adhesion, and Freeze-Tolerance for Multi-Environmental Wearable Bioelectronic Devices, *Chem. Mater.*, 2024, **36**, 4456–4467.

84 X. Yao, S. Zhang, L. Qian, N. Wei, V. Nica, S. Coseri and F. Han, Super stretchable, self-healing, adhesive ionic conductive hydrogels based on tailor-made ionic liquid

for high-performance strain sensors, *Adv. Funct. Mater.*, 2022, **32**(33), 2204565.

85 P. Li, H. Zong, G. Li, Z. Shi, X. Yu, K. Zhang, P. Xia, S. Yan and J. Yin, Building a Poly (amino acid)/Chitosan-Based Self-Healing Hydrogel via Host–Guest Interaction for Cartilage Regeneration, *ACS Biomater. Sci. Eng.*, 2023, **9**(8), 4855–4866.

86 D. C. Tuncaboylu, M. Sari, W. Oppermann and O. Okay, Tough and self-healing hydrogels formed via hydrophobic interactions, *Macromolecules*, 2011, **44**(12), 4997–5005.

87 D. Lu, Q. Lian and M. Zhu, Bioinspired Multistimuli-Induced Synergistic Changes in Color and Shape of Hydrogel and Actuator Based on Fluorescent Microgels, *Adv. Sci.*, 2024, **11**(3), 2304776.

88 M. Nakahata, Y. Takashima, H. Yamaguchi and A. Harada, Redox-responsive self-healing materials formed from host–guest polymers, *Nat. Commun.*, 2011, **2**(1), 511.

89 D. Lu, M. Zhu, J. Jin and B. R. Saunders, Triply-responsive OEG-based microgels and hydrogels: regulation of swelling ratio, volume phase transition temperatures and mechanical properties, *Polym. Chem.*, 2021, **12**(30), 4406–4417.

90 P. D. Thornton, R. J. Mart and R. V. Ulijn, Enzyme-responsive polymer hydrogel particles for controlled release, *Adv. Mater.*, 2007, **19**(9), 1252–1256.

91 P. Basu, N. Saha, T. Saha and P. Saha, Polymeric hydrogel based systems for vaccine delivery: A review, *Polymer*, 2021, **230**, 124088.

92 D. Lu, M. Zhu, S. Wu, Q. Lian, W. Wang, D. Adlam, J. A. Hoyland and B. R. Saunders, Programmed multiresponsive hydrogel assemblies with light-tunable mechanical properties, actuation, and fluorescence, *Adv. Funct. Mater.*, 2020, **30**(11), 1909359.

93 D. Lu, M. Zhu, X. Li, Z. Zhu, X. Lin, C. F. Guo and X. Xiang, Thermosensitive hydrogel-based, high performance flexible sensors for multi-functional e-skins, *J. Mater. Chem. A*, 2023, **11**(34), 18247–18261.

94 Z. Li, Y. Li, C. Chen and Y. Cheng, Magnetic-responsive hydrogels: From strategic design to biomedical applications, *J. Controlled Release*, 2021, **335**, 541–556.

95 S. J. Kim, S. J. Park, I. Y. Kim, M. S. Shin and S. I. Kim, Electric stimuli responses to poly (vinyl alcohol)/chitosan interpenetrating polymer network hydrogel in NaCl solutions, *J. Appl. Polym. Sci.*, 2002, **86**(9), 2285–2289.

96 Y. Zhou, G. Liu and S. Guo, Advances in ultrasound-responsive hydrogels for biomedical applications, *J. Mater. Chem. B*, 2022, **10**(21), 3947–3958.

97 J. Li and D. J. Mooney, Designing hydrogels for controlled drug delivery, *Nat. Rev. Mater.*, 2016, **1**(12), 1–17.

98 S. Yue, H. He, B. Li and T. Hou, Hydrogel as a biomaterial for bone tissue engineering: A review, *J. Nanomater.*, 2020, **10**(8), 1511.

99 J. Lenz, F. Del Giudice, F. R. Geisenhof, F. Winterer and R. T. Weitz, Vertical, electrolyte-gated organic transistors show continuous operation in the MA cm^{-2} regime and artificial synaptic behaviour, *Nat. Nanotechnol.*, 2019, **14**(6), 579–585.

100 S. Kushida, E. Smarsly, K. Yoshinaga, I. Wacker, Y. Yamamoto, R. R. Schröder and U. H. Bunz, Fast Response Organic Supramolecular Transistors Utilizing In-Situ π-Ion Gels, *Adv. Mater.*, 2021, **33**(4), 2006061.

101 Y. Fu, L.-a. Kong, Y. Chen, J. Wang, C. Qian, Y. Yuan, J. Sun, Y. Gao and Q. Wan, Flexible neuromorphic architectures based on self-supported multiterminal organic transistors, *ACS Appl. Mater. Interfaces*, 2018, **10**(31), 26443–26450.

102 Q. Liu, Y. Liu, J. Li, C. Lau, F. Wu, A. Zhang, Z. Li, M. Chen, H. Fu and J. Draper, Fully printed all-solid-state organic flexible artificial synapse for neuromorphic computing, *ACS Appl. Mater. Interfaces*, 2019, **11**(18), 16749–16757.

103 Y. Zhao, S. Song, X. Ren, J. Zhang, Q. Lin and Y. Zhao, Supramolecular adhesive hydrogels for tissue engineering applications, *Chem. Rev.*, 2022, **122**(6), 5604–5640.

104 Y. Zhang, Q. Chen, Z. Dai, Y. Dai, F. Xia and X. Zhang, Nanocomposite adhesive hydrogels: from design to application, *J. Mater. Chem. B*, 2021, **9**(3), 585–593.

105 S. Li, Y. Cong and J. Fu, Tissue adhesive hydrogel bioelectronics, *J. Mater. Chem. B*, 2021, **9**(22), 4423–4443.

106 X. Di, Y. Kang, F. Li, R. Yao, Q. Chen, C. Hang, Y. Xu, Y. Wang, P. Sun and G. Wu, Poly (N-isopropylacrylamide)/polydopamine/clay nanocomposite hydrogels with stretchability, conductivity, and dual light-and thermo-responsive bending and adhesive properties, *Colloids Surf., B*, 2019, **177**, 149–159.

107 Q. Lu, D. X. Oh, Y. Lee, Y. Jho, D. S. Hwang and H. Zeng, Nanomechanics of cation–π interactions in aqueous solution, *Angew. Chem., Int. Ed.*, 2013, **125**(14), 4036–4040.

108 C. Cea, G. D. Spyropoulos, P. Jastrzebska-Perfect, J. J. Ferrero, J. N. Gelinas and D. Khodagholy, Enhancement-mode ion-based transistor as a comprehensive interface and real-time processing unit for in vivo electrophysiology, *Nat. Mater.*, 2020, **19**(6), 679–686.

109 K. Guo, S. Wustoni, A. Koklu, E. Díaz-Galicia, M. Moser, A. Hama, A. A. Alqahtani, A. N. Ahmad, F. S. Alhamlan and M. Shuaib, Rapid single-molecule detection of COVID-19 and MERS antigens via nanobody-functionalized organic electrochemical transistors, *Nat. Biomed. Eng.*, 2021, **5**(7), 666–677.

110 N. Li, Y. Li, Z. Cheng, Y. Liu, Y. Dai, S. Kang, S. Li, N. Shan, S. Wai and A. Ziaja, Bioadhesive polymer semiconductors and transistors for intimate biointerfaces, *Science*, 2023, **381**(6658), 686–693.

111 J. Rivnay, H. Wang, L. Fenno, K. Deisseroth and G. G. Malliaras, Next-generation probes, particles, and proteins for neural interfacing, *Sci. Adv.*, 2017, **3**(6), e1601649.

112 X. Fan, B. Xu, S. Liu, C. Cui, J. Wang and F. Yan, Transfer-printed PEDOT: PSS electrodes using mild acids for high conductivity and improved stability with application to flexible organic solar cells, *ACS Appl. Mater. Interfaces*, 2016, **8**(22), 14029–14036.

113 T. Sekitani and T. Someya, Stretchable, large-area organic electronics, *Adv. Mater.*, 2010, **22**(20), 2228–2246.

114 S. Zhang, H. Ling, Y. Chen, Q. Cui, J. Ni, X. Wang, M. C. Hartel, X. Meng, K. Lee, J. Lee, W. Sun, H. Lin, S. Emaminejad, S. Ahadian, N. Ashammakhi, M. R. Dokmeci and A. Khademhosseini, Hydrogel-enabled transfer-printing of conducting polymer films for soft organic bioelectronics, *Adv. Funct. Mater.*, 2020, **30**(6), 1906016.

115 M. Wang, Y. Luo, T. Wang, C. Wan, L. Pan, S. Pan, K. He, A. Neo and X. Chen, Artificial skin perception, *Adv. Mater.*, 2021, **33**(19), 2003014.

116 X. Fan, W. Nie, H. Tsai, N. Wang, H. Huang, Y. Cheng, R. Wen, L. Ma, F. Yan and Y. Xia, PEDOT: PSS for flexible and stretchable electronics: modifications, strategies, and applications, *Adv. Sci.*, 2019, **6**(19), 1900813.

117 D.-H. Kim, N. Lu, R. Ma, Y.-S. Kim, R.-H. Kim, S. Wang, J. Wu, S. M. Won, H. Tao and A. Islam, Epidermal electronics, *Science*, 2011, **333**(6044), 838–843.

118 Y. Li, N. Wang, A. Yang, H. Ling and F. Yan, Biomimicking stretchable organic electrochemical transistor, *Adv. Electron. Mater.*, 2019, **5**(10), 1900566.

119 Y. Dai, S. Dai, N. Li, Y. Li, M. Moser, J. Strzalka, A. Prominski, Y. Liu, Q. Zhang, S. Li, H. Hu, W. Liu, S. Chatterji, P. Cheng, B. Tian, I. McCulloch, J. Xu and S. Wang, Stretchable redox-active semiconducting polymers for high-performance organic electrochemical transistors, *Adv. Mater.*, 2022, **34**(23), 2201178.

120 Y. Fang, X. Yang, Y. Lin, J. Shi, A. Prominski, C. Clayton, E. Ostroff and B. Tian, Dissecting biological and synthetic soft–hard interfaces for tissue-like systems, *Chem. Rev.*, 2021, **122**(5), 5233–5276.

121 I. R. Minev, P. Musienko, A. Hirsch, Q. Barraud, N. Wenger, E. M. Moraud, J. Gandar, M. Capogrosso, T. Milekovic and L. Asboth, Electronic dura mater for long-term multimodal neural interfaces, *Science*, 2015, **347**(6218), 159–163.

122 P. Gu, L. Lu, X. Yang, Z. Hu, X. Zhang, Z. Sun, X. Liang, M. Liu, Q. Sun, J. Huang and G. Zu, Highly Stretchable Semiconducting Aerogel Films for High-Performance Flexible Electronics, *Adv. Funct. Mater.*, 2024, 2400589.

123 S. E. Doris, A. Pierre and R. A. Street, Dynamic and tunable threshold voltage in organic electrochemical transistors, *Adv. Mater.*, 2018, **30**(15), 1706757.

124 D. A. Bernards, D. J. Macaya, M. Nikolou, J. A. DeFranco, S. Takamatsu and G. G. Malliaras, Enzymatic sensing with organic electrochemical transistors, *J. Mater. Chem.*, 2008, **18**(1), 116–120.

125 I. Gualandi, D. Tonelli, F. Mariani, E. Scavetta, M. Marzocchi and B. Fraboni, Selective detection of dopamine with an all PEDOT: PSS organic electrochemical transistor, *Sci. Rep.*, 2016, **6**, 35419.

126 M. Ghittorelli, L. Lingstedt, P. Romele, N. I. Crăciun, Z. M. Kovács-Vajna, P. W. Blom and F. Torricelli, High-sensitivity ion detection at low voltages with current-driven organic electrochemical transistors, *Nat. Commun.*, 2018, **9**(1), 1441.

127 D. Majak, J. Fan and M. Gupta, Fully 3D printed OECT based logic gate for detection of cation type and concentration, *Sens. Actuators, B*, 2019, **286**, 111–118.

128 D. A. Koutsouras, K. Lieberth, F. Torricelli, P. Gkoupidenis and P. W. Blom, Selective ion detection with integrated organic electrochemical transistors, *Adv. Mater. Technol.*, 2021, **6**(12), 2100591.

129 C. Liao, C. Mak, M. Zhang, H. L. Chan and F. Yan, Flexible organic electrochemical transistors for highly selective enzyme biosensors and used for saliva testing, *Adv. Mater.*, 2015, **27**(4), 676–681.

130 S. Demuru, J. Kim, M. El Chazli, S. Bruce, M. Dupertuis, P.-A. Binz, M. Saubade, C. Lafaye and D. Briand, Antibody-coated wearable organic electrochemical transistors for cortisol detection in human sweat, *ACS Sens.*, 2022, **7**(9), 2721–2731.

131 E. Macchia, M. Ghittorelli, F. Torricelli and L. Torsi, in Organic electrochemical transistor immuno-sensor operating at the femto-molar limit of detection, *IEEE International Workshop on Advances in Sensors and Interfaces*, IEEE, 2017, pp 68–72.

132 J. Fan, A. A. F. Pico and M. Gupta, A functionalization study of aerosol jet printed organic electrochemical transistors (OECTs) for glucose detection, *Mater. Adv.*, 2021, **2**(22), 7445–7455.

133 R. R. Nair, Glucose sensing and hybrid instrumentation based on printed organic electrochemical transistors, *Flex. Print. Electron.*, 2020, **5**(1), 015001.

134 V. Druet, P. D. Nayak, A. Koklu, D. Ohayon, A. Hama, X. Chen, M. Moser, I. McCulloch and S. Inal, Operation mechanism of n-type organic electronic metabolite sensors, *Adv. Electron. Mater.*, 2022, **8**(10), 2200065.

135 Z. Zhou, X. Wu, T. L. D. Tam, C. G. Tang, S. Chen, K. Hou, T. Li, Q. He, J. J. Sit and J. Xu, Highly Stable Ladder-Type Conjugated Polymer Based Organic Electrochemical Transistors for Low Power and Signal Processing-Free Surface Electromyogram Triggered Robotic Hand Control, *Adv. Funct. Mater.*, 2024, **34**(1), 2305780.

136 J. E. Tyrrell, K. Petkos, E. M. Drakakis, M. G. Boutelle and A. J. Campbell, Organic Electrochemical Transistor Common-Source Amplifier for Electrophysiological Measurements, *Adv. Funct. Mater.*, 2021, **31**(33), 2103385.

137 A. Yang, J. Song, H. Liu, Z. Zhao, L. Li and F. Yan, Wearable Organic Electrochemical Transistor Array for Skin-Surface Electrocardiogram Mapping Above a Human Heart, *Adv. Funct. Mater.*, 2023, **33**(17), 2215037.

138 S. S. Andersen, A. D. Jackson and T. Heimburg, Towards a thermodynamic theory of nerve pulse propagation, *Prog. Neurobiol.*, 2009, **88**(2), 104–113.

139 S. Singh, J. Dodt, P. Volkers, E. Hethershaw, H. Philippou, V. Ivaskevicius, D. Imhof, J. Oldenburg and A. Biswas, Structure functional insights into calcium binding during the activation of coagulation factor XIII A, *Sci. Rep.*, 2019, **9**(1), 11324.

140 F. J. He and G. A. MacGregor, A comprehensive review on salt and health and current experience of worldwide salt reduction programmes, *J. Hum. Hypertens.*, 2009, **23**(6), 363–384.

141 R. Giridharagopal, L. Flagg, J. Harrison, M. Ziffer, J. Onorato, C. Luscombe and D. Ginger, Electrochemical

strain microscopy probes morphology-induced variations in ion uptake and performance in organic electrochemical transistors, *Nat. Mater.*, 2017, **16**(7), 737–742.

142 Z. Szigeti, T. Vigassy, E. Bakker and E. Pretsch, Approaches to improving the lower detection limit of polymeric membrane ion-selective electrodes, *Electroanalysis*, 2006, **18**(13-14), 1254–1265.

143 S. T. Keene, D. Fogarty, R. Cooke, C. D. Casadevall, A. Salleo and O. Parlak, Wearable organic electrochemical transistor patch for multiplexed sensing of calcium and ammonium ions from human perspiration, *Adv. Healthcare Mater.*, 2019, **8**(24), 1901321.

144 Z. Mousavi, A. Ekholm, J. Bobacka and A. Ivaska, Ion-selective organic electrochemical junction transistors based on poly (3, 4-ethylenedioxythiophene) doped with poly (styrene sulfonate), *Electroanalysis*, 2009, **21**(3-5), 472–479.

145 J. Liao, H. Si, X. Zhang and S. Lin, Functional sensing interfaces of PEDOT: PSS organic electrochemical transistors for chemical and biological sensors: a mini review, *Sensors*, 2019, **19**(2), 218.

146 H. Tang, P. Lin, H. L. Chan and F. Yan, Highly sensitive dopamine biosensors based on organic electrochemical transistors, *Biosens. Bioelectron.*, 2011, **26**(11), 4559–4563.

147 I. Gualandi, M. Marzocchi, E. Scavetta, M. Calienni, A. Bonfiglio and B. Fraboni, A simple all-PEDOT: PSS electrochemical transistor for ascorbic acid sensing, *J. Mater. Chem. B*, 2015, **3**(33), 6753–6762.

148 D. Arcangeli, I. Gualandi, F. Mariani, M. Tessarolo, F. Ceccardi, F. Decataldo, F. Melandri, D. Tonelli, B. Fraboni and E. Scavetta, Smart bandaid integrated with fully textile OECT for uric acid real-time monitoring in wound exudate, *ACS Sens.*, 2023, **8**(4), 1593–1608.

149 X. Xi, D. Wu, W. Ji, S. Zhang, W. Tang, Y. Su, X. Guo and R. Liu, Manipulating the sensitivity and selectivity of OECT-based biosensors via the surface engineering of carbon cloth gate electrodes, *Adv. Funct. Mater.*, 2020, **30**(4), 1905361.

150 X. Ma, H. Chen, P. Zhang, M. C. Hartel, X. Cao, S. E. Diltemiz, Q. Zhang, J. Iqbal, N. R. de Barros and L. Liu, OFET and OECT, two types of Organic Thin-Film Transistor used in glucose and DNA biosensors: A Review, *IEEE Sens. J.*, 2022, **22**(12), 11405–11414.

151 C. Liao, M. Zhang, L. Niu, Z. Zheng and F. Yan, Highly selective and sensitive glucose sensors based on organic electrochemical transistors with graphene-modified gate electrodes, *J. Mater. Chem. B*, 2013, **1**(31), 3820–3829.

152 L. J. Currano, F. C. Sage, M. Hagedon, L. Hamilton, J. Patrone and K. Gerasopoulos, Wearable sensor system for detection of lactate in sweat, *Sci. Rep.*, 2018, **8**(1), 1–11.

153 J.-L. Lafuente, S. González, C. Aibar, D. Rivera, E. Avilés and J.-J. Beunza, Continuous and Non-Invasive Lactate Monitoring Techniques in Critical Care Patients, *Biosensors*, 2024, **14**(3), 148.

154 J. Ok, S. Park, Y. H. Jung and T. i. Kim, Wearable and Implantable Cortisol-Sensing Electronics for Stress Monitoring, *Adv. Mater.*, 2024, **36**(1), 2211595.

155 L. Zhang, G. Wang, C. Xiong, L. Zheng, J. He, Y. Ding, H. Lu, G. Zhang, K. Cho and L. Qiu, Chirality detection of amino acid enantiomers by organic electrochemical transistor, *J. Biosens. Bioelectron.*, 2018, **105**, 121–128.

156 G. Dhawan, G. Sumana and B. Malhotra, Recent developments in urea biosensors, *Biochem. Eng. J.*, 2009, **44**(1), 42–52.

157 P. Cirillo, W. Sato, S. Reungjui, M. Heinig, M. Gersch, Y. Sautin, T. Nakagawa and R. J. Johnson, Uric acid, the metabolic syndrome, and renal disease, *J. Am. Soc. Nephrol.*, 2006, **17**(12_suppl_3), S165–S168.

158 S. C. Howard, C.-H. Pui and R. C. Ribeiro, Tumor Lysis Syndrome, *Renal Disease in Cancer Patients*, 2014, pp. 39–64.

159 M. Heinig and R. J. Johnson, Role of uric acid in hypertension, renal disease, and metabolic syndrome, *Cleve. Clin. Q.*, 2006, **73**(12), 1059.

160 A. Gilletti and J. Muthuswamy, Brain micromotion around implants in the rodent somatosensory cortex, *J. Neural Eng.*, 2006, **3**(3), 189.

161 B. Schmatz, A. W. Lang and J. R. Reynolds, Fully printed organic electrochemical transistors from green solvents, *Adv. Funct. Mater.*, 2019, **29**(44), 1905266.

162 M. Afonso, J. Morgado and L. Alcácer, Inkjet printed organic electrochemical transistors with highly conducting polymer electrolytes, *J. Appl. Phys.*, 2016, **120**(16), 165502.

163 T. Ye, J. Wang, Y. Jiao, L. Li, E. He, L. Wang, Y. Li, Y. Yun, D. Li and J. Lu, A tissue-like soft all-hydrogel battery, *Adv. Mater.*, 2022, **34**(4), 2105120.

164 P. Yang, J.-L. Yang, K. Liu and H. J. Fan, Hydrogels enable future smart batteries, *ACS Nano*, 2022, **16**(10), 15528–15536.

165 S. Huang, L. Hou, T. Li, Y. Jiao and P. Wu, Antifreezing hydrogel electrolyte with ternary hydrogen bonding for high-performance zinc-ion batteries, *Adv. Mater.*, 2022, **34**(14), 2110140.

166 A. Khazaeli, G. Godbille-Cardona and D. P. Barz, A Novel Flexible Hybrid Battery–Supercapacitor Based on a Self-Assembled Vanadium-Graphene Hydrogel, *Adv. Funct. Mater.*, 2020, **30**(21), 1910738.

167 Z. Chen, J. W. To, C. Wang, Z. Lu, N. Liu, A. Chortos, L. Pan, F. Wei, Y. Cui and Z. Bao, A three-dimensionally interconnected carbon nanotube–conducting polymer hydrogel network for high-performance flexible battery electrodes, *Adv. Energy Mater.*, 2014, **4**(12), 1400207.

168 D. Jiang, N. Lu, L. Li, H. Zhang, J. Luan and G. Wang, A highly compressible hydrogel electrolyte for flexible Zn-MnO2 battery, *J. Colloid Interface Sci.*, 2022, **608**, 1619–1626.

169 L. Li, B. Fang, D. Ren, L. Fu, Y. Zhou, C. Yang, F. Zhang, X. Feng, L. Wang and X. He, Thermal-switchable, trifunctional ceramic–hydrogel nanocomposites enable full-lifecycle security in practical battery systems, *ACS Nano*, 2022, **16**(7), 10729–10741.